Development and characterization of sensitive, energy-independent solid-state photon dosemeters with high spatial and temporal resolution. Applications in clinical radiology and radiation protection.

Herrnsdorf, Lars

2018

Document Version:
Publisher's PDF, also known as Version of record

Development and characterization of sensitive, energy-independent solid-state photon dosemeters with high spatial and temporal resolution

Applications in clinical radiology and radiation protection

LARS HERRNSDORF
MEDICAL RADIATION PHYSICS MALMÖ | LUND UNIVERSITY

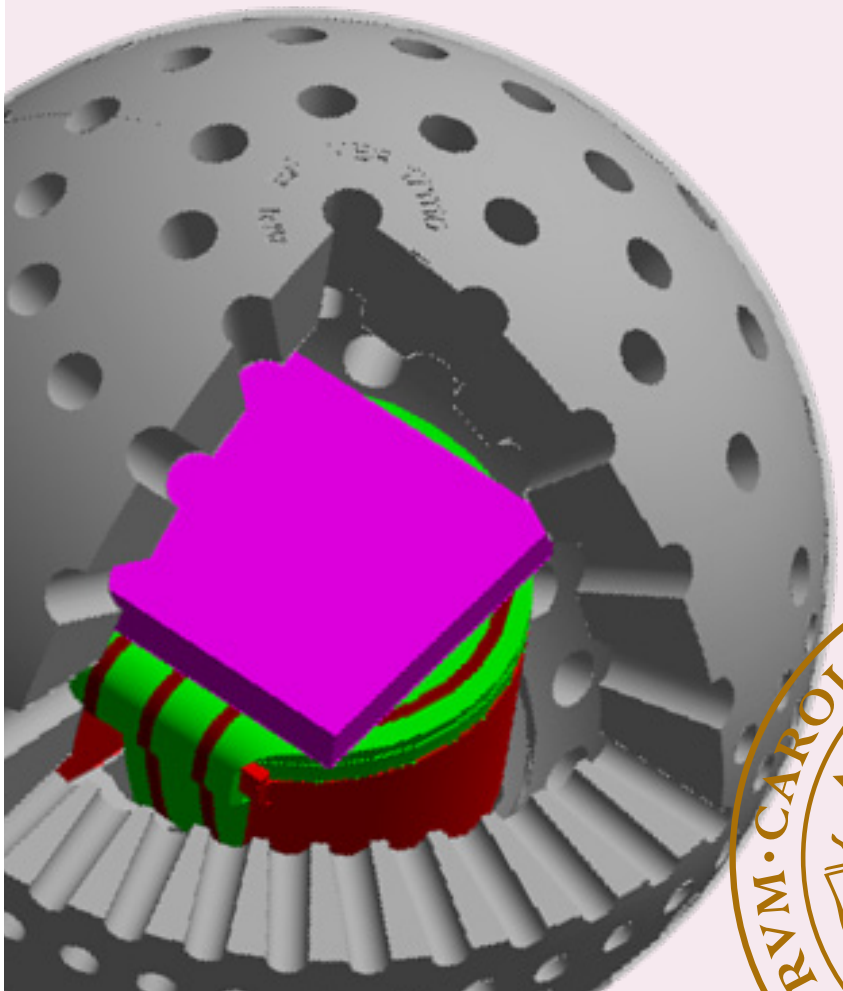

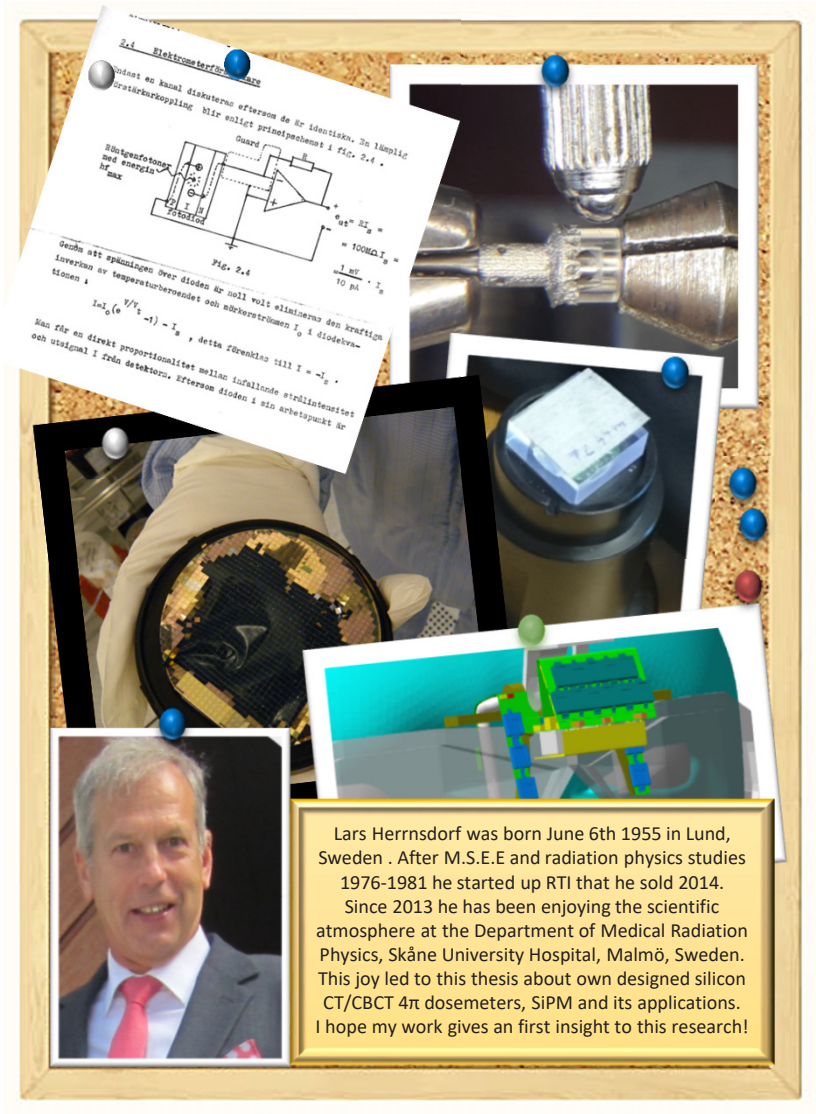

Department of Translational Medicine
Medical Radiation Physics Malmö
Skåne University Hospital

Lund University, Faculty of Medicine
Doctoral Dissertation Series 2018:82
ISBN 978-91-7619-648-9
ISSN 1652-8220

FACULTY OF MEDICINE

LUND UNIVERSITY

Printed by Media-Tryck, Lund 2018 NORDIC SWAN ECOLABEL 3041 0903

Development and characterization of sensitive, energy-independent, solid-state photon dosemeters with high spatial and temporal resolution

Applications in clinical radiology and radiation protection

Lars Herrnsdorf

LUND
UNIVERSITY

DOCTORAL DISSERTATION
by due permission of the Faculty of Medicine, Lund University, Sweden.
To be defended in Lilla Aulan, Medicinskt forskningscentrum (MFC), Jan Waldenströms gata 5, ingång 59, Skånes Universitetssjukhus i Malmö, 2018-06-08, 09:15

Faculty opponent
Ass. professor Hans Bornefalk,
KTH Royal Institute of Technology, Stockholm

Organization LUND UNIVERSITY	Document name DOCTORAL DISSERTATION
	Date of issue 2018-06-08
Author(s) Lars Herrnsdorf	Sponsoring organization

Title and subtitle:
Development and characterization of sensitive, energy-independent, solid-state photon dosemeters with high spatial and temporal resolution
Applications in clinical radiology and radiation protection

Abstract

Modern medicine and health care rely on a variety of diagnostic and therapeutic equipment and methods that involve ionizing radiation. To guarantee quality and the safety of patients and staff, advanced radiation detectors and dosemeters are needed that have low energy and operate with directional independence for X-ray and γ-ray photons. Similar instruments are also of great importance for measurements used in radiation protection and safety outside of hospitals and the health care sector and for nuclear and radiological emergencies.

In this thesis, new sensors, detectors, and dosemeters based on silicon were designed, manufactured, characterized, and tested.

The aim was to develop dosemeters with signals that are as independent as possible of the energy and direction of the incoming X-ray and γ-ray photons. Starting with a 350 µm silicon wafer, a sensor was constructed with electrical contacts on one side only. A flex card was adapted with anisotropic conductive adhesive (ACA) and mounted to the sensor. Since all components have low X-ray attenuation, the disturbance of the radiation field by the detector is minimal from all directions.

Another important component is the metal filter encapsulating the silicon detector. Made of stainless steel, this encompassing filter compensates for the energy and directional variation of sensitivity of the silicon detector. The filter was designed using a series of Monte Carlo calculations. The hole pattern was selected so that the signal (proportional to the absorbed dose) was independent of the X-ray source position (in 4π). Due to the small structures, additive manufacturing (AM) in the form of metal 3D printing was needed to fabricate the filter.

The functionality of the 4π dosemeter was verified by simulation to meet the quality criterion that the energy dependence is less than 5% for the IEC beam qualities RQR and RQT in the range 65–145 kV. The best way to microfabricate the sensor, sensor holder, flex card, and energy filter was evaluated and a method to control its mounting accuracy is proposed.

The application of silicon detectors in radiology (CT, CBCT, and planar radiography) was tested, and a specific dosemeter construction also was tested for eye lens dosimetry and for emergency situations.

To broaden the use of silicon detectors in future medical imaging and dosimetry applications, an overview of silicon photomultipliers (SiPM) for this area is included and a learning and training program targeted to graduate students is described.

Keywords: Si PIN, sensor, detector, dosemeter, CT, CBCT, dose profile, CTDP, R100, SiPM, Medipix, MCNP, AM, 4π detector, ACA, flex card micro assembly

Classification system and/or index terms (if any)

Supplementary bibliographical information		Language: English
ISSN and key title		ISBN 978-91-7619-648-9
Recipient's notes	Number of pages 77	Price
	Security classification	

Signature Lars Herrnsdorf Date 2018-05-03

Development and characterization of sensitive, energy-independent, solid-state photon dosemeters with high spatial and temporal resolution

Applications in clinical radiology and radiation protection

Lars Herrnsdorf

LUND
UNIVERSITY

A doctoral thesis at a university in Sweden takes either the form of a single, cohesive research study (monograph) or a summary of research papers (compilation thesis) which the doctoral student has written alone or together with one or several other author(s).

In the latter case, the thesis consists of two parts. An introductory text puts the research work into context and summarizes the main points of the paper. Then, the research publications themselves are reproduced together with a description of the individual contributions of the authors. The research papers may either have been already published or are manuscripts at various stages (in press, submitted, or in draft).

Front cover: 4π dosemeter head. Illustration by Lars Herrnsdorf.

Back cover: bulletin board version of the thesis. Illustration by Jan Lindström.

Department of Translational Medicine
Medical Radiation Physics Malmö
Skåne University Hospital
SE-205 02 Malmö, Sweden

Lund University, Faculty of Medicine Doctoral Dissertation Series 2018:82
ISSN 1652-8220
ISBN 978-91-7619-648-9

Printed in Sweden by Media-Tryck, Lund University, Lund 2018

Maria, because you made it possible. You are constantly present though you are physically gone.

Jeanie, because you are so wise and having the ability to move on and share my life.

My three children, Johan, Karin and Maja who proved the value of having a family.

Content

List of figures

19. The S12572-010C boasts a resolution of 90,000 individual avalanche photo diodes (APD) on a 3 mm x 3 mm wafer die, with a pixel pitch of 10 µm. This SIPM is used in **VII** when a high dynamic range is preferred over sensitivity, as is the case with the sensitivity especially needed to measure X-rays.
20. LH2424 PIN sensor. (Left) 2.40 mm x 2.40 mm from contact side. (Right) Sketch describing the structure and the layers needed to make an electrical contact via the use of ACP and the thin flex card.
21. (Left) Flex card at the sensor side with the 5 contact points. (Right) Microscope image of a LH2424 sensor where the ACP small Au bumps can be seen (8–20 µm size).
22. Demonstration example to show the importance of selecting the right hole pattern to reduce energy dependence.
23. The evolution from the basic two-dimensional energy filter to an increasingly sophisticated version of the 3D 4π energy filter in IV.
24. Optimized energy and angular filter. (Left) CAD model. (Middle) 3D printed version of the 4π dosemeter. (Right) Dosemeter assembly parts: “Head” part of the filter, sensor mounted on the flex card, detector holder, and “neck” part of the energy filter (IV
25. (1)The dosemeter without 4π energy filter: (a) bare sensor, (b) with a thin filter mounted on both sides (VI). (2) 4π dosemeter within a CT/CBCT assembly. (3) 4π dosemeter as a reference detector.
26. Assembly of the sensor with flex card detector holder and energy filter. Assembly of the sensor with flex card detector holder and energy filter. A, B, C, D, and E refer to Table 3. (Left) The energy filters with two parts put together. (Right) The nominal dimensions indicated in mm. The pink rectangle is the sensor that can partly be seen in the opened segment of the sphere's mantle surface. See also Figure 24 for an additional image of the parts inside the 4π energy filter.
27. 0.5 µm resolution contactless microscope. (Left) The structure of the neck energy wall. (Right) The measurement resolution is 1.5752 mm for the sample 3 of the neck energy inner dimension (marked with a red circle in the figure) (see Table 3).
28. (Left top) PMMA detector holder, neck part of energy filter. A guide pin is shown to align (right) the detector holder and the neck part using a watchmaker lathe and a dial indicator to glue the parts together. (Left down) The setup to mill the detector holder to its final height and flatness on the neck part of the energy filter. The precision of this micro milling equipment is within 0.5 µm. (Right down) An image of the cylindric guide rod that fits the square sensor precisely and guides the sensor with its flex card in the center of the detector holder.
29. Left:Sensor and flex card after glued to the detector holder and the flex card mounted inside the neck part. Right: The head and neck part joined together. The diameter of the head part is nominally 7.00 mm.
30. Application with SIPM for measurements of pulse height distributions from scintillators, intensifying screens and for luminince dosemeters as OSL.
31. Comparison between an old 1 x 1 mm^2 Hamamatsu SiPM (model S10362-11-025C) (upper picture) and a new 1.3 × 1.3 mm^2 Hamamatsu SiPM (model S13360 -1350CS) (lower picture).
32. Drone inspection with mobile battery operated 4π dosemeter or/and SiPM alpha/beta/gamma/neutron spectrometer/dosemeter.
33. The real time personal dosemeter based on a Si-sensor described in VI In this application the thin sensor and flexcard is placed inside the phantom where normally only TLD and OSL could be placed.
34. 4π dosemeter for QC of CT- and CBCT-units. Monte Carlo driven control of the dose to patient and personnel in an X-ray room.
35. Virtual KAP meter. The left figure displays a set up in a CT were the dose is measured in, 0˚,90˚,180˚ and 270˚ position simultenously around a body anthropomorphic phantom using a Barracuda multi channel electrometer (RTI Group). For the lowest dosemeter (0˚), that is the only one needed, the doserate vaweform is displayed on the right picture. The CT is rotating one turn per second so the the time between the dosemeter doserate pulses is 500 ms.

Abbreviations

4π	The solid angle of a complete sphere measured in steradians
AAPM	American Association of Physicists in Medicine
ABC	Automatic brightness control
ACA	Anisotropic conductive adhesive
ACF	Anisotropic conductive film
ACP	Anisotropic conductive paste
ADC	Analog-to-digital converter
Al_2O_3	Aluminium oxide
AM	Additive manufacturing
APD	Avalanche photo diode
ASIC	Application specific integrated circuit
Au	Gold (atomic number 79)
BGA	Ball grid array
BGO	Bismuth germanium oxid
CAD	Computer-aided design
CAM	Computer added manufacturing
CBCT	Cone beam CT
CdTe	Cadmium telluride
CT	Computed tomography
CTDIvol	Volume computed tomography dose index
CTDP	CT dose profiler
CTH	Chalmers University of Technology
DAP	Dose area product
DR	Digital radiography
E	Effective dose
EFR	Energy filter version R
EF07	Energy filter version 07
ESS	European spallation source in Lund
FWHM	Full width at half maximum
HVL	Half value layer
IAEA	International Atomic Energy Agency
ICRP	International Commission on Radiological Protection
IEC	International Electrotechnical Commission
KAP	Kerma area product

LED	Light-emitting diode
LH2424	PIN sensor used in 4π detector
LTH	Lund University, Faculty of engineering
LU	Lund University
LYSO	Lutetium-yttrium oxyorthosilicate
MAXIV	Synchrotron radiation facility in Lund,
MC2	Department of microtechnology and nanoscience CTH
MCA	Multichannel analyzer
MCNP	Monte Carlo N-particle code
MEDIPIX	Multi-pixel photon counter
MPPC	Multi-pixel photon counter=SiPM
O-ARM	Intraoperative X-ray imaging system
ORAMED	Optimization of radiation protection for medical staff.
OSL	Optically stimulated luminescence
PCB	Printed circuit board
PET/MR	Positron emission tomography–magnetic resonance imaging
PIN DIODE	A diode with a wide, undoped intrinsic semiconductor region between a p-type semiconductor and an n-type semiconductor region
PMMA	Polymethyl methacrylate
PMT	Photomultiplier tube
QA	Quality assurance
QC	Quality control
ROI	Region of interest
RQC	Radiation qualities based on copper added filter for ABC system
RQR	Radiation qualities in radiation beams emerging from the X-ray source assembly
RQT	Radiation qualities based on copper added filter for CT system
RQX	IEC 61267 beam quality standard: either RQR, RQT or RQC
R100	Radiation dose detector
RTI2424	PIN sensor used in CTDP
SGC	Saint-Gobain Crystals
Si	Silicon (atomic number 14)
SiPM	Silicon photo multiplier
SSD	Source skin distance
Ti	Titanium (atomic number 22)
TiN	Titanium nitride
TLD	Thermoluminescent dosemeter

Original papers

This thesis is based on the following seven publications, which will be referred to by their Roman numerals:

I. Measurement of the sensitive profile in a solid state silicon detector, irradiated by X-rays. Thungström G, **Herrnsdorf L**, Norlin B, Reza S, Krapohl D, Mattsson S, Gunnarsson M.14th International Workshop on Radiation Imaging Detectors, 1–5 July 2012, Figueira da Foz, Portugal. *Jinst Published by IOP Publishing for Sissa Medialab, April 4, 2013*

II. Silicon diode as an alpha particle detector and spectrometer for direct field measurements. Ören Ü, Nilsson J, **Herrnsdorf L**, Rääf CL, Mattsson S. *Radiat. Prot. Dosim.* 170(1–4), 247–251, 2016

III. Beam quality correction factors for KAP meters for lightly and heavily filtered X-ray beams. **Herrnsdorf L**, Peterson H. *Rad. Prot. Dosim.* 169(1-4), 347-352, 2016

IV. Optimization of energy and directional response of a small 4π silicon dosemeter for quality control of CT/CBCT-units – A 3D CAD, Monte-Carlo, AM approach. **Herrnsdorf L,** Andersson M, Gunnarsson M, Mattsson S. Manuscript submitted to *Phys. Med. Biol*, 2018

V. A method to characterize the radiation output from a cone beam O-arm using a device for dose and dose profile scanning measurement. **L Herrnsdorf,** M Söderberg. *Proceedings of SPIE, vol. 8668. Medical Imaging 2013: Physics of Medical Imaging; 86682Q; doi: 10.1117/12.2006514.*

VI. Construction and evaluation of a real time personal dosemeter based on a Si-sensor invisible to X-rays. **Herrnsdorf L**, Gunnarsson M, Mattsson S. Manuscript submitted to *Appl. Radiat. Isotop.*, 2018

VII. Silicon photomultipliers for medical imaging and dosimetry-An overview**.** **Herrnsdorf L**, Caccia M, Mattsson S. *Rad. Prot. Dosim.* 169(1-4), 430-435, 2016

Other related publications by the author

Design of an electronic penetrameter (in Swedish). Alerman H, Andersson U, **Herrnsdorf L**, Karlsson R. *B Sc thesis, 1980 Chalmers University of technology, Göteborg, Sweden*

Design and performance evaluation of a new instrument for in-beam quality control of X-ray equipment. **Herrnsdorf L,** Månsson L G, Strid K-G. *Report GU-RADFYS 84:09 (1984) Department of Radiation Physics, University of Göteborg, Sahlgenska Hospital, Göteborg, Sweden*

Average glandular dose in routine mammography screening using a Sectra Microdose mammography unit. Hemdal B, **Herrnsdorf L**, Andersson I, Bengtsson G, Heddson B, Olsson M. *Radiat. Prot. Dosim.* 114(1-3), 436–443, 2005

Point dose profile measurements using solid-state detectors in characterization of computed tomography systems. **Herrnsdorf** L, Björk M, Cederquist B, Mattsson C G, Thungström G, Fröjdh C. *Nucl. Instr. Meth. A* 607, 223–225, 2009

Absorbed dose and dose rate using the Varian OBI 1.3 and 1.4 CBCT system. Palm Å, Nilsson E, **Herrnsdorf L.** *J Appl. Clin. Med. Phys.* 11(1), 229–240, 2010

Pseudohelical scan for the dose profile measurements of 160-mm-wide cone-beam MDCT**.** Lin P-J P, **Herrnsdorf L**. *Am. J. Radiol.* 194, 897-902, 2010

A directly readable personal dosemeter for radiation emergemcy situations – A design approach. **Herrnsdorf L.** In: *Medical Physics in the Baltic States 10 (Ed. by Adlienè D), Kaunas University of Technology,* 2012, pp 23-28

Review of methods to control patient doses and image quality in various CT techniques. **Herrnsdorf L**. In: *Medical Physics in the Baltic States 10 (Ed. by Adlienè D), Kaunas University of Technology,* 2012, pp 97-98

Can an energy-compensated solid-state X-ray detector be used for radiation protection applications at higher photon energies? Ören Ü, **Herrnsdorf L**, Gunnarsson M, Mattsson S, Rääf C L. *Radiat. Prot. Dosim.* 169(1-4), 292-296, 2016

IDAC-CAD2VOX - A software for radiation protection calculations for the ICRP reference phantoms which are in an environment described by detailed CAD drawings. Andersson M, **Herrnsdorf L**, Mattsson S. In: *Medical Physics in the Baltic States 13 (Ed. by Adlienè D), Kaunas University of Technology*, 2017, pp 10-13

Patents

X-ray detection device for CT dose profile measurements.
Lars Herrnsdorf, Björn Cederquist, Tomas Bengtsson
WO 2010/140944 A1, EP 2438465 B1

A method for determining alignment of light and an X-ray fields of an X-ray apparatus
Lars Herrnsdorf
WO 2010/132002 A1

Device and method of imaging or measuring of a radiation source
Lars Herrnsdorf. WO 95/14941014941 A1, US 5872830A

Oral presentations/Posters:

Initial study of a CT QA-method to determine spatial variation in X-ray focus position (flying focus and collimation) and CT gantry vibrations. **Herrnsdorf L.** European Congress of Radiology, 2006, poster C-699, *www.springerlink.com/index/1t1n335631618u07*

Evaluation of a PCB design in order to minimize the X-ray scatter for a solid state silicon detector. **Herrnsdorf L,** Thungström G. Poster at Sensible Things that Communicate, STC-expo, Sundsvall, October 2012

Project description of a micro fabricated flip-chip solid state silicon detector/PCB design with and without ACF. Experimental equipment and model. External resources and contact network. **L. Herrnsdorf** Medical Radiation Physics Malmö, Lund University and Department of Microtechnology and Nanoscience, MC2, Chalmers University of Technology, Gothenburg

Dosimetric measurements using the TG 200 phantom – a comparison of dosimetric techniques with application in CT and CBCT. Gunnarsson M, **Herrnsdorf L**, Törnqvist P, Söderberg M. Optimisation in X-ray and molecular imaging, 4th Malmö Conference on medical imaging, Gothenburg, 28-30 May 2015

Introducing postgraduate education for silicon photomultipliers (SiPM) and other solid state technologies based on a modular kit for experimental training. **Herrnsdorf L**, Mattsson S. Optimisation in X-ray and molecular imaging, 4th Malmö Conference on medical imaging, Gothenburg, 28-30 May 2015

Summary

Modern medicine and health care rely on a variety of diagnostic and therapeutic equipment and methods that involve ionizing radiation. To guarantee quality and the safety of patients and staff, advanced radiation detectors and dosemeters are needed that have low energy and operate with directional independence for X-ray and γ-ray photons. Similar instruments are also of great importance for measurements used in radiation protection and safety outside of hospitals and the health care sector and for nuclear and radiological emergencies.

In this thesis, new sensors, detectors, and dosemeters based on silicon have been designed, manufactured, characterized, and tested.

The aim was to develop dosemeters with signals that are as independent as possible of the energy and direction of the incoming X-ray and γ-ray photons. Starting with a 350 μm silicon wafer, a sensor was constructed with electrical contacts on one side only. A flex card was adapted with anisotropic conductive adhesive (ACA) and mounted to the sensor. Since all components have low X-ray attenuation, the disturbance of the radiation field by the detector is minimal from all directions.

Another important component is the metal filter encapsulating the silicon detector. Made of stainless steel, this encompassing filter compensates for the energy and directional variation of sensitivity of the silicon detector. The filter was designed using a series of Monte Carlo calculations. The hole pattern was selected so that the signal (proportional to the absorbed dose) was similar independently of the X-ray source position (in 4π). Due to the small structures, additive manufacturing (AM) in the form of metal 3D printing was needed to fabricate the filter.

The functionality of the 4π dosemeter was verified by simulation to meet the quality criterion that the energy dependence is less than 5% for the IEC beam qualities RQR and RQT in the range 65–145 kV. The best way to microfabricate the sensor, sensor holder, flex card, and energy filter was evaluated and a method to control its mounting accuracy is proposed.

The application of silicon detectors in radiology (CT, CBCT, and planar radiography) was tested, and a specific dosemeter construction also was tested for eye lens dosimetry and for emergency situations.

To broaden the use of silicon detectors in future medical imaging and dosimetry applications, an overview of silicon photomultipliers (SiPM) for this area is included and a learning and training program targeted to graduate students is described.

Populärvetenskaplig sammanfattning

Joniserande strålning uppfattas ofta som något mystiskt. Den kan inte ses eller höras, den luktar intet. Men strålning finns överallt runt oss och vi utsätts för den dagligen under våra liv. Det ät troligt att strålningen haft en avgörande inverkan på jordens och människans utveckling. Men när strålningsnivåerna överstiger de nivåer för vilka människor är anpassade kan det bli problem i form av såväl direkta vävnadsskador som ökad cancerutveckling. Därför behövs strålningsmätning och övervakning, som i sin tur kräver känsliga och pålitliga instrument.

Strålningsdosimetri handlar om den exakta bestämningen av strålningsenergin avsatt i olika material, såsom levande vävnad. Hur strålningen interagerar med materialet bestäms av typen av strålning och dess energi samt materialets täthet och sammansättning. Detta gör strålningsdosimetrin komplex och det behövs nya och bättre detektorer och dosimetrar. Här ger kiselbaserade halvledardetektorer nya möjligheter.

Denna avhandlings röda tråd handlar om att utveckla millimeterstora kiselelement som byggs ihop till detektorer och slutligen till dosimetrar för strålningsmätning. Särskilda krav ställs på utformning av de material som finns runt kiselelementet.

Ett nytt sätt presenteras att utforma dosmätaren så att den har samma mätkänslighet oberoende av strålningens riktning, energi och styrka. Kombination av snabbhet och liten volym gör att dosmätaren med fördel kan användas för kontroll av datortomografer (CT eller skiktröntgenutrustning) där stålningen från ett röntgenrör kommer från alla håll och dess dosprofil skall kunna mätas på endast delar av en sekund. Genom att utforma ett klotformat filter av metall med noga avpassade hål uppnår man de egenskaper som behövs. Då CT undersökningar ger jämförelsevis stora dosbidrag till patienterna är detta en viktig tillämpning.

Denna avhandling börjar med att från en kiselkristall som används i ett renrum framställa millimeterstora sensorer från kiselskivor (ni ser en sådan skiva på baksidan på avhandlingen) för att sedan utforma detektorerna till färdiga dosmätare för användning inom sjukvård, omgivning och för mätningar vid strålningsolyckor.

I arbete I beskrivs en metod att mäta upp den strålningskänsliga volymen hos sensorn vilket är viktigt då inte hela kiselvolymen är stålningskänslig. Denna information användes sedan för att göra en beräkning av hur man optimalt skall utforma kapslingen runt kiselelementet beroende på applikation.

I arbete II användes kiselelementet utan kapsling. Detta gör att även en alfa-partikel kan komma in i detektorn. Syftet var att ta en enkel och bärbar variant av detektorn som kan användas för att detektera alfastrålning spektrometriskt, och dess energi för att kunna särskilja alfastrålande radionuklider. Tillämpningar är mätningar på hud och kläder på personer på en skadeplats och i öppna sår och på hud hos patienter som skadats.

Arbete III och V visar på tillämpningar där QA strålningsmätningar utförs med krav på konstant mätkänslighet och att det är snabba nog att hinna med att återge strålning intensitet då röntgenrörets högspänning slås på och av samtidigt som bilddetektor fotograferar patienten för att skapa digitala röntgenbilder.

Tyngdpunkten i arbete VI visar på hur man kan ansluta kiselelement med en speciellt tunn elektriskt ledande pasta och ett tunt flexibelt kretskort så att man kan få en väldigt tunn och platt detektor som inte syns på röntgen men ändå har tillräckligt känslighet för att mäta t.ex. personalstråldoser och kan placeras i närheten av organ som t.ex. ögonlinsen.

Den stora utmaningen i arbete IV är att finna en ett optimalt utformat klotformat metallfilter som omsluter sensorn och dess elektriska anslutningar från alla håll. På framsidan av avhandlingen finns en bild på denna så kallade 4π dosmätare med ett kiselelement i mitten. Förutsättningarna för detta bygger på erfarenheter från arbete I, III och V och att man i datorn tar fram en modell baserad på så kallad Monte Carlo teknik. Med denna teknik kan man följa strålningens väg från röntgenröret fram till detektorn och beräkna den del av strålningen som absorberas i mätvolym och ger upphov till en signal. På detta sätt kan olika kombinationer av filtertjocklek och hålstorlek testas.

Med hjälp av en 3D skrivare som kan skriva ut godtycklig form direkt i rostfritt stål kan sedan metalfiltret skapas och testas experimentell.

Det har varit en utmaning att montera ihop alla små delar pga. små toleranser och små dimensioner. Det klotformade hålfiltret är endast 7 mm i diameter och detektorn skall kunna monteras inuti denna samtidigt som den skall fungera elektriskt med sina anslutningar. Därför finns förslag till monteringsrutiner i avhandlingen.

I arbete VII presenteras en ny typ av kiseldetektor (SiPM) med inbyggd förstärkning som utnyttjar egenskaper som gör att enskilda ljusfotoner kan mätas enkelt, detta öppnar nya möjligheter för mätningarna och är inte bara ett komplement till vanliga kiseldetektorerna. Arbetet visas på hur denna typ av detektor kan kombineras med en scintillator som omvandlar joniserande strålning till ljus och på så sätt kan användas för att detektera strålning och dess energi. En applikation som redan finns är användningen av detektorer i positronemissionstomografi (PET) kameror och som dosmätare för strålskyddsinstrument.

Introduction and background

Modern medicine and health care rely on a variety of diagnostic and therapeutic equipment and procedures that involve ionizing radiation (Rehani *et al.* 2011). Advanced radiation detection technology is needed to ensure that the equipment and methods used are of high quality and are safe for both patients and staff. (Mattsson 2016) Radiation detector measurements are also important for radiation protection in other fields under normal and emergency situations.

Radiation dosimetry addresses the accurate determination of radiation energy deposited in different materials, such as living tissue. The interaction of the radiation with the material is determined by the type of radiation and its energy as well as the density and composition of the material. Thus, radiation dosimetry is complex and interdisciplinary, and there is a constant need for new and better detectors and dosemeters. For example, silicon-based detectors are now being applied to estimate radiation effects in human tissue (Bengtsson and Herrnsdorf 2013).

Dosimetry of ionizing radiation is essential to quality assurance in medicine. Thus, it is not surprising that virtually all effects that can be attributed to ionizing radiation have been used for dosimetry. For example, dosemeters can be based on ionization in air or other gases or in solid-state materials (e.g., silicon).

Table 1 lists different radiation effects and associated dosimetric techniques.

Table 1. Radiation detectors for dosimetry.

Effect	Dosemeter	Quanty/Unit	Examples of specific instruments	Used in
Physical effect				
Ionization in gases	Air ionization chamber	Absorbed dose/Gy	NE 2530 30 cm^3 and FC65-G Farmer 0.6 cm^3	**III, V**
	CT pencil chamber	Dose length/Gy cm	Radcal 10x6-3CT 10 cm long,0.3 cm^3	**V**
	KAP chamber	Kerma area product/$Gycm^2$	PTW Diamentor M4, 20 x20 x 1.58 cm^3	**V**
	Proportional counter			
	Geiger Müller tube			
Ionization in liquids	Liquid filled ionization chamber	Absorbed dose/Gy		
Ionization in solids	Semiconductor silicon PIN dosemeter	Absorbed dose/Gy	X-ray analyzer, R100, LH2424	**I, II, III, IV, V, VI**
	CTDP dose profile detector	Absorbed dose/Gy	RTI2424 1.2 mm^3 mounted in a Ø 12.5 mm Al tube	**IV, V**
	Alpha spectrometer		RTI2424 1.2 mm^3 +3 µm Mylar foil window	**II**
	4π reference Si-detector	Absorbed dose/Gy	LH2424 1.2 mm^3 +energy filter Ø 7 mm stainless steel	**IV**
	Real- time personal dosemeter	Absorbed dose/Gy Personal dose equivalent/Sv	LH2424 1.2 mm^3 +angle filter 0.2 mm flex card	**VI**
	Avalanche photo diode (APD)		Component in SIPM	**VII**
	Beta, gamma spectrometer		SIPM Hamamatsu S10362-33-050C, 3 x 3 mm^2	**VII**
Lumine-scence	Thermo luminescence dosemeter (TLD)	Absorbed dose/Gy		**VI**
	Optical stimulated luminescence dosemeter (OSL)	Absorbed dose/Gy		
Fluore-scence	Gd_2O_2S:(Pr) Scintillators, light field/X-ray field alignment, X-ray waveform		RTI Nova 40x40 cm^2 screen with video camera, Hamamatsu S12572-010P, 3 x 3 mm^2	**III, VII**
	LYSO(Ce), BGO, CsI(Tl), other scintillators		SGC 3x3x15 mm^3 optical connected to SIPM	**VII**
	Electron paramagnetic resonance (EPR)	Absorbed dose/Gy		
Chemical effect				
Fricke dosimetry	**Transformation of Fe^{2+} to Fe^{3+}**	**Absorbed dose/Gy**		
Chemical transitions	Radiographic film Radiochromic film	Absorbed dose/Gy		
Chemical dosimetry	Gel dosimetry Calorimetry	Absorbed dose/Gy	SIPM S12572-010P, 3 x 3 mm^2	
Biological effect				
	Erythema Chromosome damage DNA damage			

Dosemeters can be passive or active. Passive dosemeters collect energy when exposed to a radiation field, and they do not provide a signal until they are processed to extract the desired latent information. Active dosemeters, however, provide continuous data that can be used immediately or stored for future analysis.

Because of this continuous measurement property, active dosemeters are advantageous in radiation therapy and for diagnostic applications as they provide an understanding of the time course and spatial distribution of the absorbed dose delivery to patients. (Lin and Herrnsdorf 2010) For radiation protection applications, active dosimetry enables changes to be made to procedures and positions in the room or in the environment in order to reduce the absorbed dose. This is not possible with passive dosemeters that are read after the exposure. Similar needs exist in radiation emergency situations, and access to a directly readable rugged dosemeter for first-line rescue personnel has long been a priority. Personnel at risk of exposure need immediate information about their absorbed dose rate so they can plan the next step in their work to maximize safety.

Modern solid-state technology presents a novel approach to dosemeters. Silicon dosemeters can be made small and they have low power consumption as well as a high temporal resolution. Furthermore, silicon dosemeters have much higher sensitivity (around a factor of 5000) than ion chambers (Figure 1).

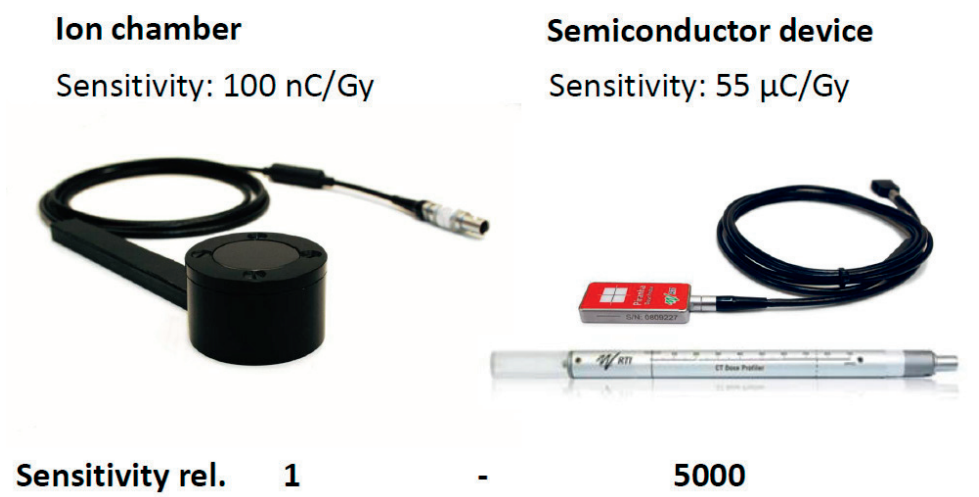

Figure 1. Comparison of the sensitivity of two detectors.
(Left) A 3000 mm3 flat air ionization chamber. (Right, top): A 35 mm3 solid-state detector with 2D energy filter. (Right, bottom): A 2.1 mm3 solid-state detector with an RTI2424 sensor.

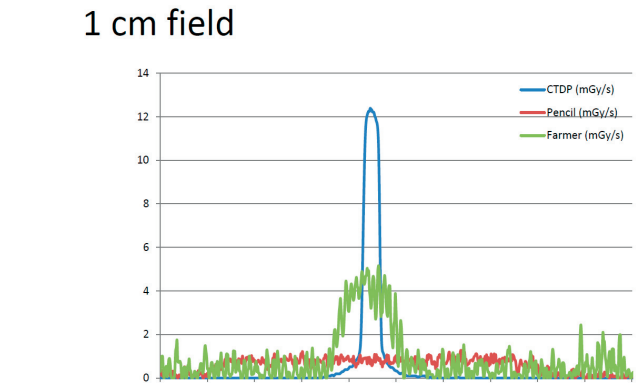

Overview

Beam width	Dose (mGy)		
	CTDP	Pencil	Farmer
160 mm	111	108	111
100 mm	74	75	74
60 mm	43	50	43
40 mm	28	31	27
20 mm	13,4	15,6	13,1
10 mm	5,2	6,0	5,3
5 mm	2,9	3,2	2,9
2,5 mm	1,0	0,44	0,40

Beam width	Peak Doserate (mGy/s)		
	CTDP	Pencil	Farmer
160 mm	15	15	15
100 mm	15	12	15
60 mm	14,5	7	14,5
40 mm	14	5	12,5
20 mm	13,5	2	10
10 mm	12,5	0,8	4
5 mm	11,5	0,5	2
2,5 mm	10	?	?

Figure 2.
(Top) Signal from three dosemeters scanned over a 10 mm wide X-ray beam. The active length of the dosemeters was 0.3 mm (CTDP RTI2424), 100 mm (10x6-3CT Pencil) and 23.1 mm (FC65-G Farmer). (Bottom) Table of accumulated dose and peak dose rate when the three dosemeters were scanned simultaneously in various wide beams from 160 mm down to 2.5 mm, as measured with a 3-channel Barracuda system (RTI Group, Mölndal, Sweden).

This factor of 5000 allows devices to be made smaller, more sensitive, and/or able to compensate for disadvantages such as energy dependence, etc.

The small size of silicon detectors allows measurements to be made with high spatial resolution.

A small detector (active volume = 1.2 mm3) can correctly follow the true dose profile with high sensitivity. This is illustrated in the left part of Figure 2, where three different dosemeters are scanned simultaneously through a 10 mm wide X-ray beam.

Comparing the use of an ion chamber with a semiconductor detector, the smaller size and higher time resolution of the semiconductor results in a difference in the peak dose rate up to a factor of 30. For correct measurements of the peak dose rate for small objects, such as eyes, the selection of a small dosemeter is vital (Figure 2).

Silicon sensor materials have the disadvantage that they have a pronounced dependence on the photon energy in the diagnostic X-ray range.

However, there is an opportunity to overcome this disadvantage because of their high sensitivity, as various attenuation materials can be used to partly cover the sensor area. Figure 3 graphically describes a 2D solution in which a silicon detector provides an energy independent response that is also independent of radiation quality in the X-ray range (Lindström 2016, RTI 2010). When the energy is increased, more of the X-rays penetrate the energy filter, resulting in an increased "active sensor area". In this way, the increased sensor area compensates for the signal drop at higher energies (Figure 3).

For an increasing number of applications, there is a need for 3D dose measurements. Here, the challenge is to extend this energy correction principle to a 4π detector that also eliminates directional dependence.

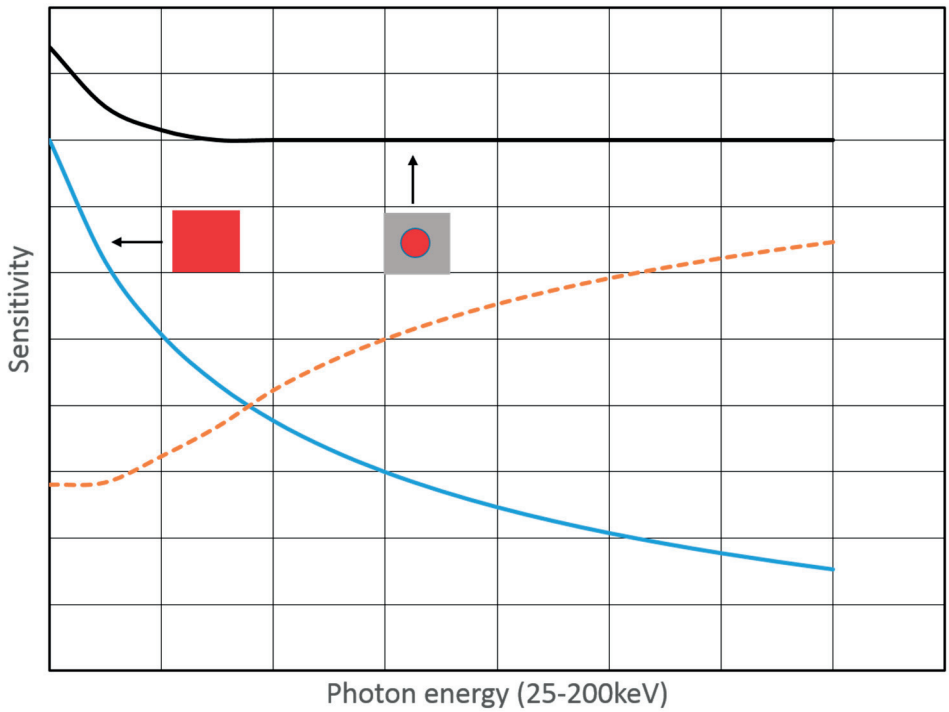

Figure 3. Principal illustration of the method used to compensate for the high sensitivity with low energy photons in silicon.
The image to the left illustrates a 10x10 mm2 silicon sensor and the one to the right shows the same sensor covered by a metal filter with a round hole in the middle. When the energy is increased, more and more of the X-rays penetrate the energy filter so that the "active sensor area" (dotted line) is increased.

A 4π dosemeter and an appropriate electrometer have increasing applications in fields where the dose level is high and a uniform angular response is needed. These include QA of CT/CBCT and tomosynthesis units, verification of Monte Carlo calculations in the dose estimation for patients and personnel in health care, and radiation protection in connection with nuclear and radiological accidents.

Of all artificial radiation sources, those used in medicine contribute the largest doses to the human population. Among X-ray and nuclear medicine diagnostics, computer tomography (CT) contributes 70% of the total collective effective dose (EU 2014).

A CT examination exposes patients to a higher dose (by an order of magnitude) than corresponding conventional examinations; therefore, quality control is important and should be measured regularly.

The drastic evolution of CT/CBCT, from small field and single slices to more than 160 mm and 256 slices, has created a demand for new and improved methods (Boone 2011, IEC 2012a, 2012b, ICRP 2015,) for dosimetry, safety, and acceptance tests, as illustrated in Figure 4.

The IEC standards now also accept small size dosemeters, in addition to pencil chambers that measure dose length (IEC 2012).

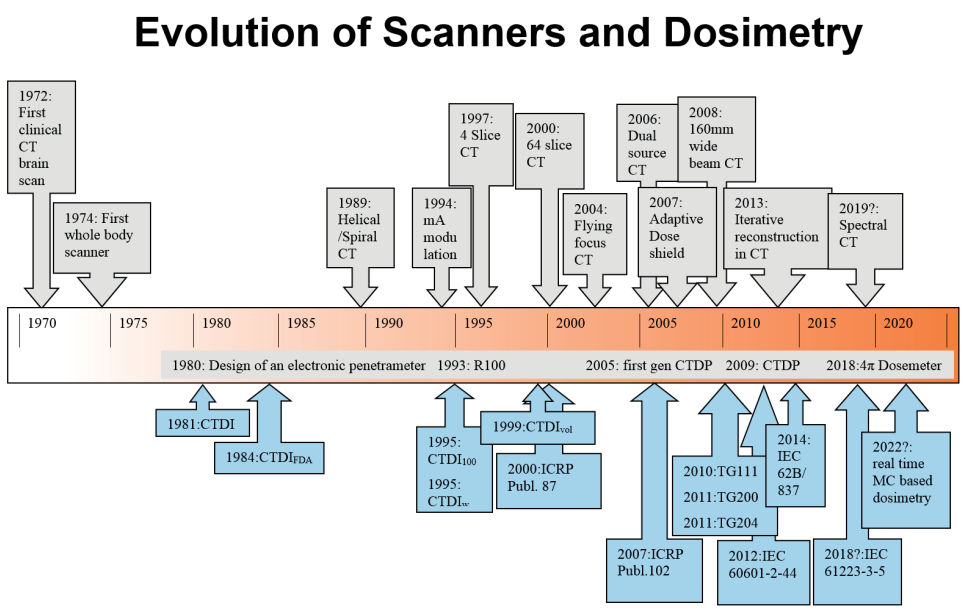

Figure 4. Evolution of CT scanners and dosimetry 1970-2018. Modified from Boone (2011).

Advances in microelectronics allow for the creation of ever more sophisticated structures in the front-end electronics of modern imaging equipment. (Persson *et al.* 2014) This evolution makes it possible to design "noise-free" detectors enabling lower dose levels, as well as the formation of "spectral images" that can result in better diagnoses (Åslund *et al.* 2007, Bornefalk and Danielsson 2010).

The new imaging technology also sets new demands for dosimetry and especially for 4π energy-independent dosemeters. To avoid artifacts for all dosemeters, it is important to reduce the amount of external material, especially high-Z components, that encapsulate the sensor itself. This can be done using modern bonding techniques (Cao *et al.* 2005). It is also important to adapt the electronics to handle a large amount of information in order to avoid overflow or pileup.

Progress in additive manufacturing (AM) methods has made it possible to produce arbitrarily shaped structures in the form of 4π filters and absorbers of high-Z material such as stainless steel (Digital metal 2018).

The parallel progress in computational power enables advanced calculation methods, such as Monte Carlo simulations, together with the voxelization of complex structures from 3D CAD drawings (Andersson *et al.* 2017).

This introduction has described the needs and possibilities for the construction of improved dosemeters with minimal energy and directional dependence.

The aims of the thesis

The ultimate aim of this thesis is to explore the potential of silicon detectors in the development of dosemeters with high spatial and temporal resolution that provide a signal per unit of absorbed dose which is independent of the energy of the photons and their direction.

- Construct silicon wafers and optimize their electrical contacts for radiation purposes (**I, II, IV, VI**).
- Construct a 3D angle flattener sensor filter for the unsymmetrical sensor element (**VI**).
- Construct a 4π energy filter that should compensate for the energy dependence of silicon alone (**IV**).
- Design a reference detector with optimal energy and angular performances, meeting the IEC standards for dose meters used in diagnostic radiology (CT, CBCT, and planar radiography) (**IV**).
- Evaluate the detector for use in spectrometry (**II**).
- Test the application of silicon detectors in radiology (CT, CBCT, and planar radiography) (**III, V**).
- Evaluate the detector for use in eye radiation protection and for emergency situations (**VI**).
- Evaluate the potential of the SiPM detector for medical imaging and dosimetry and describe a learning and training program targeted to graduate students (**VII**).
- Evaluate the best way to microfabricate the sensor, sensor holder, flex card, and energy filter and find a method to control the sensor's mounting accuracy (**IV, VI**).

Sensor response and its electronic

Response

The signal (charge or current) from the silicon sensor is produced by the absorption of photons of various energies in the active silicon. Electron/hole pairs are generated in the silicon by photoelectric absorption, compton scattering and pair production (if the energy exceeding 1.02 MeV).

In the depletion volume electrons and holes are separated by the internal electric field. In the intrinsic non depleted volume (low doped n-type), holes diffuses and when they reach the depletion volume they are swept by the electric field towards the anode. The movement of electrons and holes in the depletion volume induce charges on the electrodes, i.e. Ramos theorem. (Castoldi 2011) Normally, the active thickness is primarily determined by the depletion layer, which is a function of doping and applied voltage. In our case, without an applied external voltage to the sensor RTI2424 and LH2424, the depletion area is about 30 μm. In addition to the contribution from absorption in the depletion region, the charge signal includes a contribution from the diffusion current. With a zero-biased sensor, this contribution to the signal is major. The sensitivity is therefore related to the thickness of the intrinsic part of the sensor (Figure 5, right) and the expected gain in sensitivity based on the diffusion current.

The relative sensitivity as a function of diffusion length (Figure 5, left) across the sensor is calculated based on the sensitivity profile measurement and Equation 2.2 in I. So, even if a thicker Si wafer could increase the relative response, the effect is very minor—only a factor of 1.5 when the thickness is increased from 350 μm to 1000 μm since the signal only comes from diffusion with zero voltage over the PIN sensor. Due to costs and other reasons, a 350 μm wafer thickness with high-purity silicon was selected for the LH2424 design (Figure 5, right).

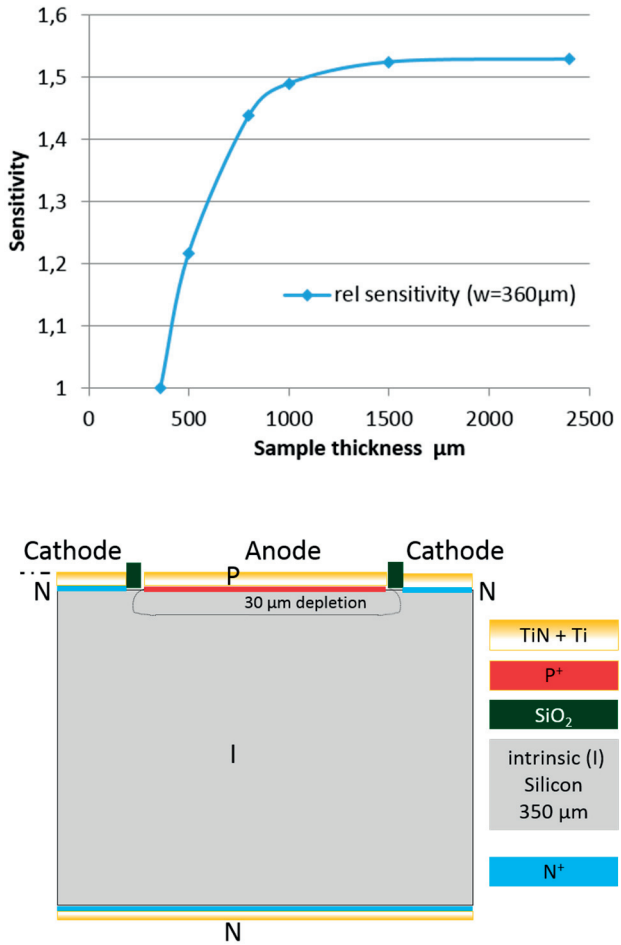

Figure 5.
(Top) Relative sensitivity of silicon as a function of thickness and (bottom) the design of LH2424 based on a of 350 µm thick PIN sensor material.

PIN "short circuit current mode" configuration

To match the performance of the sensor response, an electrometer preamplifier in "short-circuited current mode" is selected (Herrnsdorf *et al.* 1984) since it has very good performance as a dosemeter. In Figure 6, the voltage V over the sensor is equal to zero. This eliminates the impact of the dark current Io and the temperature-dependent term Vt.

V = the voltage across the anode and cathode of the PIN junction

$I = Io(e(V/Vt) - 1) + Ir$

where Ir is the current generated by radiation.

The diode equation can then be written as I = Ir, since ($e\left(\frac{V}{Vt}\right) = 1\ for\ e(0)$).

This means that a direct proportionality exists between the incoming radiation and Ir.

This linear relation is valid for 6 to 7 decades of signal level, and the lower limit is even lower than Io itself. Furthermore, the relationship is not temperature dependent. This current can be integrated during a controlled time interval t_o to create a dosemeter.

Electronic circuit

There are two types of approaches: Charge integrating devices (**I, III, IV, V, VI**) (Figure 6) and single quantum-counting devices (**II, VII**) (Figure 7-8).

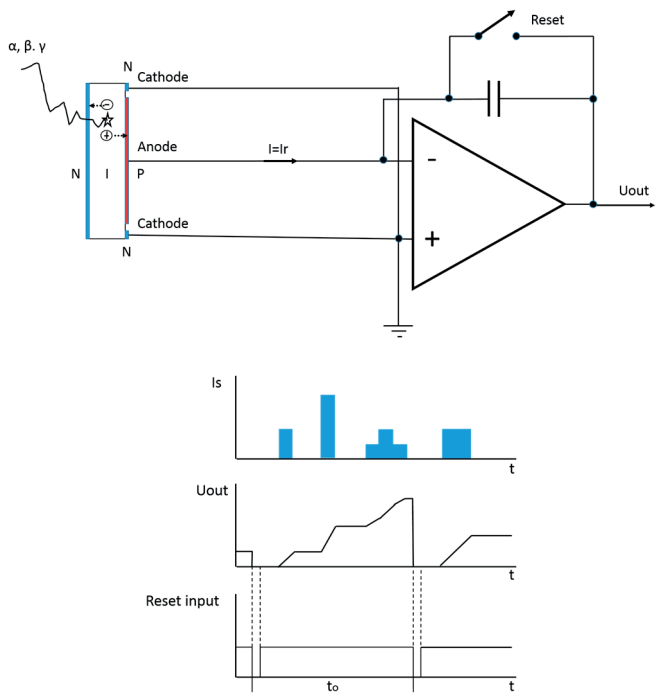

Figure 6. Illustration of a charge integration dosemeter
The sensor is connected to an integrated, time-controlled electrometer that can measure charges in small time intervals. The typical dynamical range is up to 20 bits (dynamic range 1:10^6) and the maximum sample rate of 3 kHz and current I=Ir can be measured down to 5 fA.

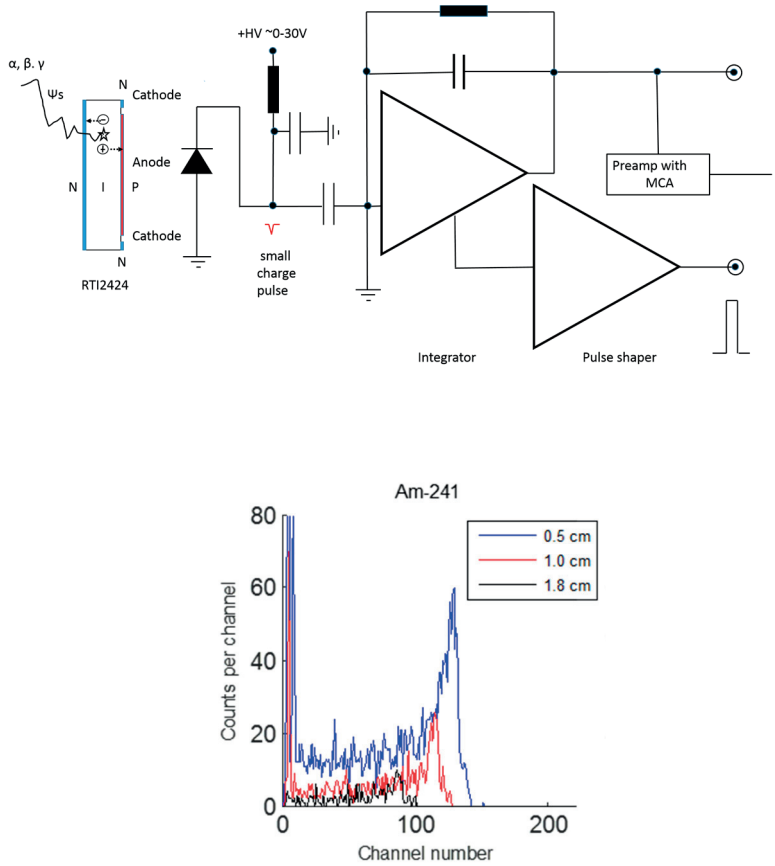

Figure 7. Illustration of a pulse mode dosemeter with internal sensor gain of 1.
The 4 mm^2 Si RTI2424 sensor connected to a charge-sensitive preamplifier in pulse mode (2003 BT) and a digital portable MCA. Pulse height distribution measured with RTI2424 sensor for an electrodeposited 241Am source (Eα= 5486 and 5443 keV) (bottom) at various SDD (0.5, 1.0, and 1.8 cm). Individual photons can be measured (pulse length in the µs range). If sophisticated ASICS with both preamplifiers and high-speed ADC/MCA are used to direct measure the charge pulse near the sensor, even high dynamic dose rate outputs from CT can be collected without pileup.

Use of APD (avalanche photo diodes) and, in its newest form, MPPC (multi-pixel photon counter), also named SiPM (silicon photo multiplier), in the new cost-effective detector construction offers new possibilities toward developing an extremely sensitive detector that can count single photons in the ns range (Figure 8). SiPMs are adapted to microprocessors and ASICS.

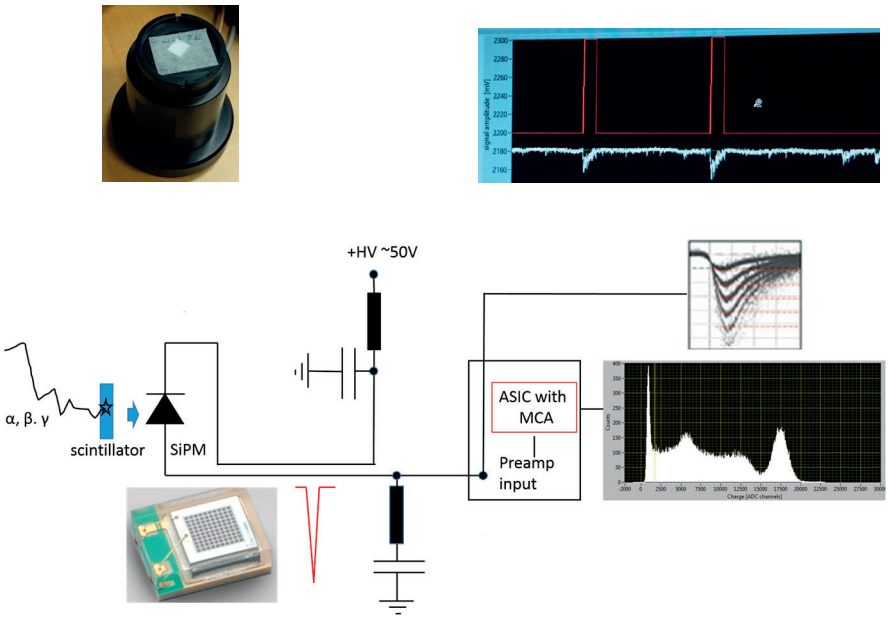

Figure 8. Illustration of a pulse mode dosimeter with an internal sensor gain of 10^5 to 10^6.
Since the internal gain is so high for the SiPM, a much simpler preamplifier can be used and the sensor is less sensitive to pickup noise. The left picture shows an experiment where a fast Gd_2O_2S:(Pr) scintillator is placed directly above the SIPM and a ^{99m}Tc- source is on top of that. The right image displays the individual photon pulses from the source.

Verification and absorption test of sensor, detector, and dosemeter

In this thesis, many of the challenges dealt with the desired ability to “see” what is going on and to obtain a deeper understanding of what is hidden to the observer. It is not enough to use eyesight or even microscopic or high-resolution diagnostic X-ray images from a body CT/CBCT. The resolution is simply insufficient. The smallest parts that must be studied are only a fraction of a µm. But, since it is also crucial for these parts to be visible using X-rays when connecting the sensors with the electrical contact in a BGA fashion, there is a need to use equipment that normally only exists in silicon manufacture cleanrooms and in material science laboratories.

The equipment used for detailed studies are the following:

- 4D imaging laboratory, Lund University, Faculty of Engineering, LTH.
- MC2 laboratory, Chalmers University of Technology, CTH, Gothenburg. Olympus microscope and FINEPLACER bonder for ACF and BGA mounting especially related to ACA (both ACF and ACP).
- 2D X-ray Micro focus laboratory, Mid Sweden University, Sundsvall. Medipix2 image spectroscopy X-rays sensor.

Their applications and uses are described in Figures 9–13.

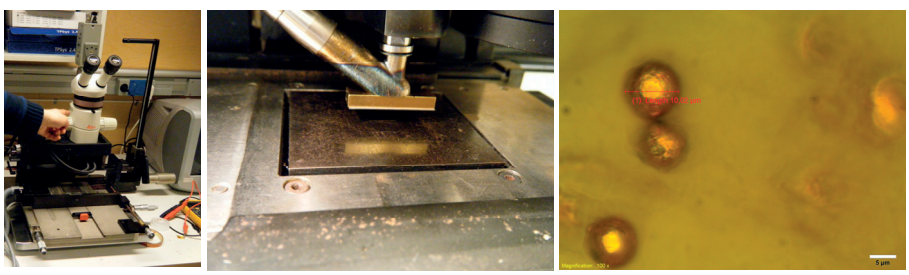

Figure 9. BGA and ACA mounting.
Finetech FINEPLACER flip-chip ACF bonder at MC2, CTH used for the investigation of the best contact and packaging method.

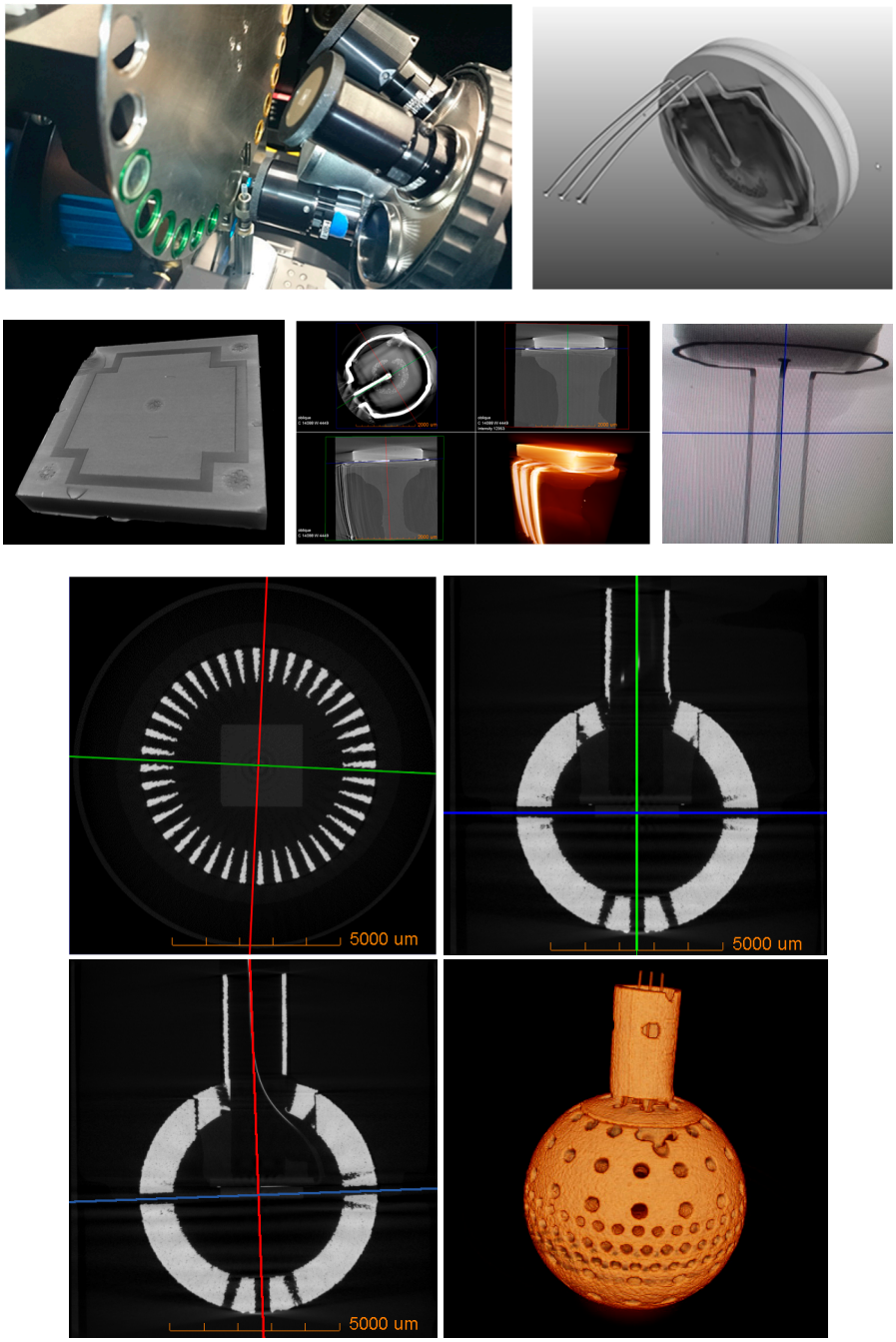

Figure 10. 4D image laboratory. Verification of sensor detector dosemeter mounting.
High-resolution X-ray tomograph for 3D imaging of the internal structure of bulk materials (Zeiss Xradia XRM520). Resolutions down to <700 nm. Detailed studies of the attenuation of the flex card, detector holder, sensor, and ACP as well as control of the alignment of sensor to the 4π energy filter.

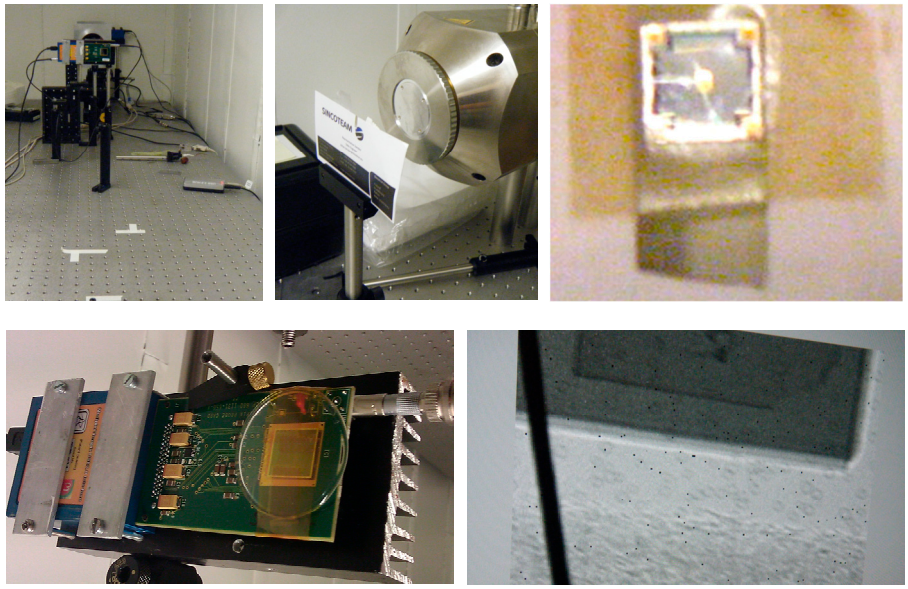

Figure 11. 2D X-ray microscopy of ACA compared to the attenuation of the sensor, gold wire and paper . (Up left) Setup with the tube in the front and the Medipix camera in the back (up middle) a business card in front of the X-ray tube act as a holder for the RTI2424 sensor, ACA and a 20 µm gold wire (up right) zoomed picture of the sensor, ACA, paper and gold wire tape together**.** (Down left) Medipix2 camera.(Down right) X-ray image from the Medipix2 camera ; the ACA compared to the other nearby attenuation materials.

Carefully study individual parts based on the micro CT pictures (Figure 10) and measure and verify the position of the sensor inside the 4π energy filter version EF07 have been of great help to define the steps needed for the micro assembly of the whole detector (Table 3).

As seen in Figure 11 (down right), the attenuation is less in the ACA region than in the piece of paper. (See also Figure 8 in **IV** for identifying the parts in the image**)** The 20 µm gold wire (black) has very high attenuation and the silicon sensor element has uniform attenuation. Furthermore, the size of the Ag-plated plastic balls is approximately 10 µm in diameter (half of the gold wire) and the X-ray image indicates that only the surface of the balls includes high-Z material. The image clearly indicates that the ACA has a negligible added effect on the attenuation and therefore enables an X-ray-invisible electrical contact method.

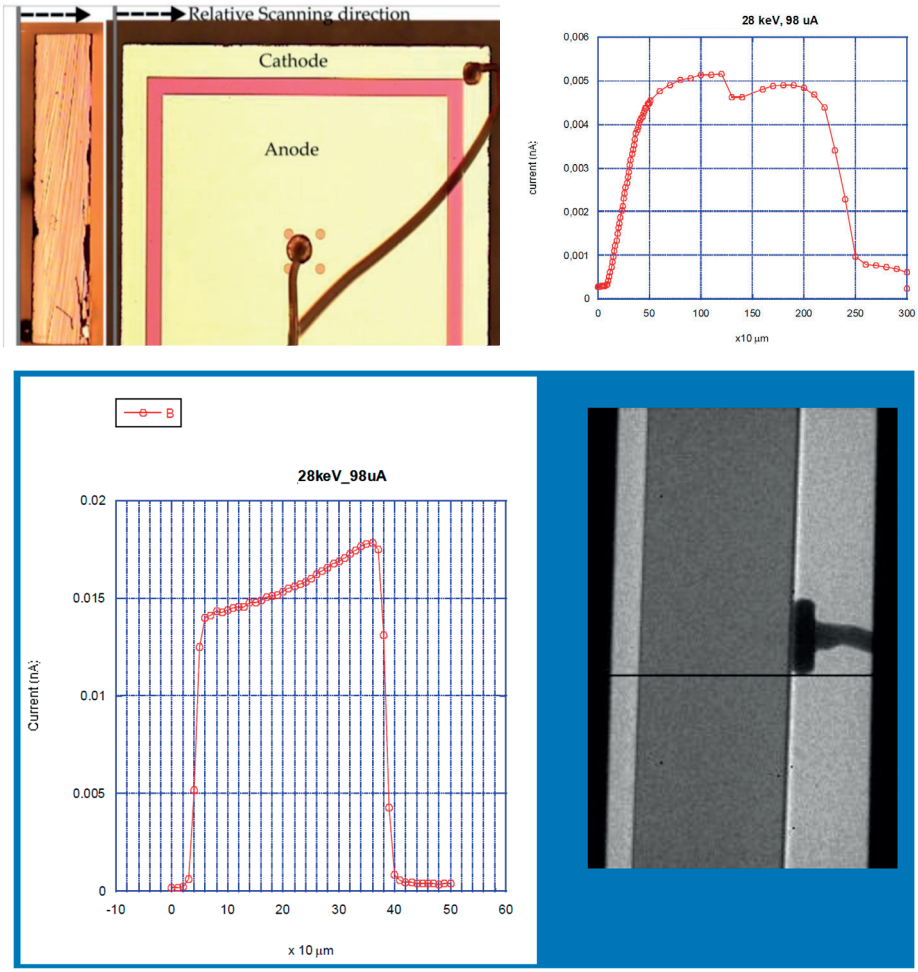

Figure 12.Sensitivity profile measurement XY and Z.
A micro focus tube and Medipix2 image detector with analyzing spectrometer software were used. The X-ray current was in the order of 100 µA and the signal to the Piranha electrometer (RTI Group) was in the order of a few fA.

Please note the high attenuation of the the wire bonding contact and how it influence the sensitivity profile (Figure 12). A sketch of the experimental setup, for the sensitivity profile measurement (Thungström *et al.* 2012) with slit plane parallel to the paper can be found in figure 1 in **I**, see also Figure 14.

An example (Figure13) of the resolution you can expect of the 4π dosemeter based on the CT scout image from a clinically used CT. This resolution is not good enough to be helpful for the design of the dosemeter compares to Figure 10 and 11.

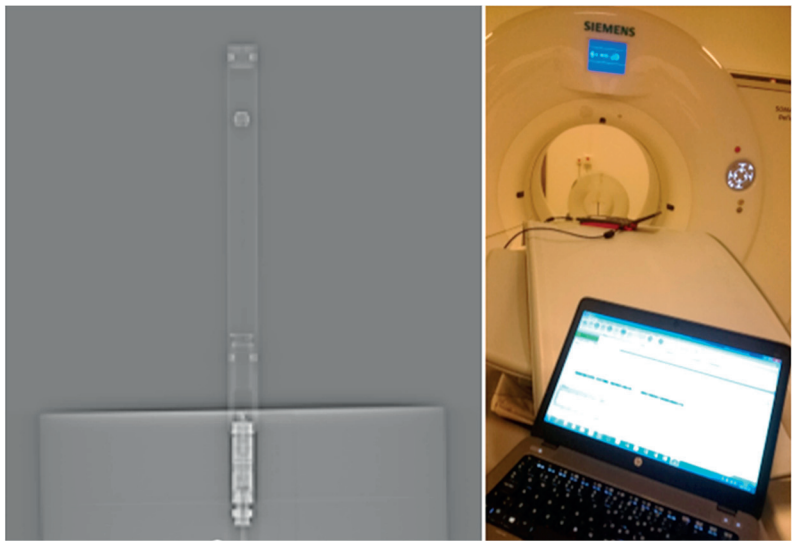

Figure 13. QA CT setup.
Scout image and measurement of the dose profile on the first version of the 4π energy filter mounted inside the CT assembly probe (Medical radiation physics Malmö).

Summary of papers

Paper I: Measurement of the sensitivity profile in a solid-state silicon detector, irradiated by X-rays

Paper I describes the sensitivity profile of the solid-state silicon dose profile detector.
The MEDIPIX2 sensor system is an excellent method for aligning an image of an X-ray slit to a sample under test. The scanning from the front to the reverse side of the detector shows a decrease in sensitivity of 20%, which indicates a minority charge carrier lifetime of 0.18 ms and a diffusion length of 460 mm. The influence of the diced edges results in a volumetric efficiency of 59%, with an active volume of 1.2 mm^2 of the total 2.1 mm^2.

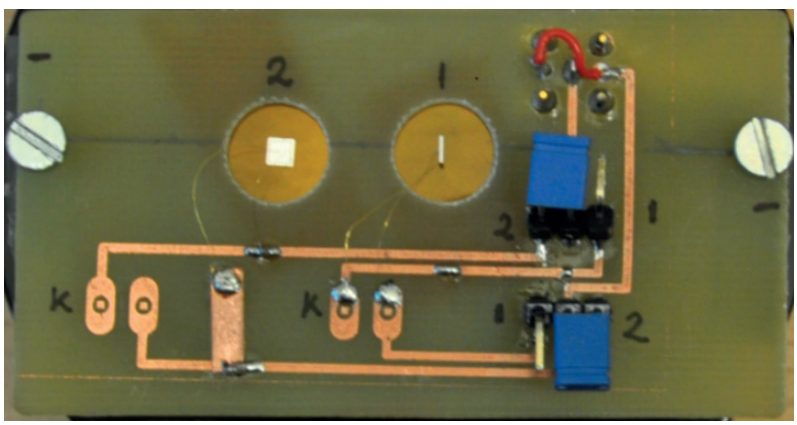

Figure 14.
A closer look at the setup of the RTI2424 sensors for measuring the sensitivity profile in **I**. The sensors are hanging free in air from thin gold wire bonding threads. The electrometer was connected to the other side of the board.

Paper II: Silicon diode as an alpha particle detector and spectrometer for direct field measurements

In paper **II**, a windowless silicon (Si) diode (4 mm^2) was evaluated as an alpha particle detector and spectrometer for field measurements. It was irradiated with alpha particles from a ^{241}Am (2.3 kBq) and a ^{210}Po (9 kBq) source at source–detector distances (SDD) of 0.5, 1.0, and 1.8 cm. The energy resolution in terms of full width at half maximum (FWHM) was 281, 148, and 113 keV for SDDs of 0.5, 1.0, and 1.8 cm, respectively. The minimum detectable activity increased from 0.08 to 0.83 Bq when the SDD increased from 0.5 to 1.8 cm. The detector has the potential for several alpha spectrometric applications, such as monitoring for wound, skin, and surface contamination at nuclear fuel facilities, nuclear power plants, and facilities handling radioactive waste. Other application areas are during environmental surveys following accidental releases of actinides in nuclear power plants and in connection with other radiological or nuclear scenarios.

Figure 15.
Dimensions of the RTI2424 to the right compared to a standard size surface barrier detector for α-spectrometry.

Paper III. Beam quality correction factors for KAP meters for lightly and heavily filtered X-ray beams

In paper III, kerma-area product (KAP) meters, which have a pronounced energy dependence when measuring air KAP for lightly filtered X-ray beams (RQR), were studied. Today, it is also common to use more heavily filtered beams (Rauch *et al.* 2012). In this work, the energy dependence for lightly as well as heavily filtered beams (RQC) was investigated for several KAP meter models. (IEC 2005) The relative energy dependence of the readings of an external and an internal KAP meter was determined relative to an ionization chamber, which had been calibrated at the primary standards laboratory. As an alternative to this measurement, an energy independent solid-state dosemeter, was used in combination with an X-ray/light field analyzer. As a complement to the measurements, the sensitivity of a KAP meter for various X-ray beam qualities was modeled using Monte Carlo simulations of photon transport and absorption. The result showed a variation in relative energy dependence of up to 30% for KAP meters for RQC beam qualities compared with RQR qualities. A reduced sensitivity of KAP meters for heavily filtered beams in comparison with lightly filtered beams was found, and it was important that the beam-specific radiation quality correction factors were applied to correct the registered KAP values.

Table 2. Calibration coefficients and correction factors for the solid state dosemeter

Beam quality Q	Calibration coefficient N_K (Gy/C)	Beam quality correction factor* k_Q	Uncertainty* U (%)
RQR3 (50 kVp, 2.5 mm Al)	$1.859 \cdot 10^4$	1.03	1
RQR5 (70 kVp, 2.8 mm Al)	$1.859 \cdot 10^4$	1	1
RQR8 (100 kVp, 3.5 mm Al)	$1.859 \cdot 10^4$	1.00	1
RQC3 (RQR3 + 0.5 mm Cu)	$1.859 \cdot 10^4$	0.93	4
RQC5 (RQR5 + 1.5 mm Cu)	$1.859 \cdot 10^4$	1.01	4
RQC8 (RQR8 + 2.0 mm Cu)	$1.859 \cdot 10^4$	1.01	4

*Uncertainty U of N_K x k_Q and beam quality correction factor k_Q are based on RTI application notes (RTI 2010).

Paper IV: Optimization of energy and directional response of a small 4π silicon dosemeter for quality control of CT/CBCT units – A 3D CAD, Monte-Carlo, AM approach

A 4π radiation dosemeter for use in medical radiology was designed. It is based on a solid-state silicon detector, a sensor wafer, a flex card, a 3D plastic holder, and a spherical stainless steel filter with a distribution of holes around the detector. The detector is attached to the wafer using only low-Z material. To achieve an energy and directional response which is as uniform as possible for various radiation qualities and beam directions, the filter was designed using a series of Monte Carlo calculations. This design is based on an earlier initial selection of hole size and thickness, and the holes are spread out around the sphere using an iterative method in which MC simulations provide feedback for changing the 3D CAD model until the results fulfill the aim. The hole pattern is designed in such a way that the energy dependence correction should be balanced over the surface so that the corresponding "active" sensor area is similarly independent of the X-ray source position (in 4π). The energy filter and its hole pattern were created using additive manufacturing (AM) in the form of metal 3D printing. The functionality of the dosimeter was verified by simulation to fulfill the quality criterion of energy dependence less than 5% for the IEC beam qualities RQR and RQT in the range of 65–145 kV.

A side view of the final detector design is shown in Figure 16.

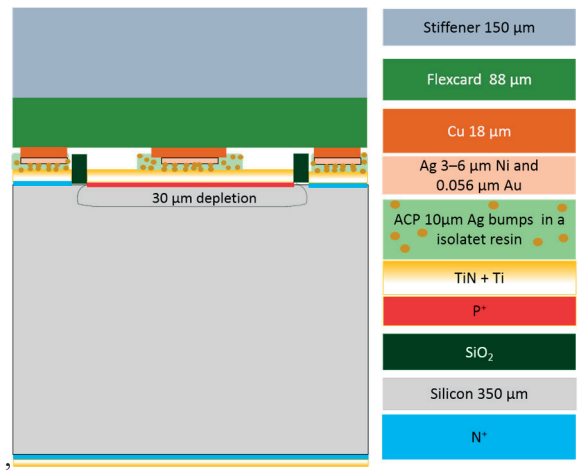

Figure 16.
The final LH2424 sensor below and on top of the sensor the ACP layer and top of that the flex card with its bumps.

Paper V: A method to characterize the radiation output from a cone beam O-arm using a device for dose and dose profile scanning measurement

The O-arm system is a mobile intraoperative DR imaging system that is composed of fluoroscopy and cone beam CT. The configuration of the O-arm system in the absence of a patient table and with a broad beam width (165 mm at isocenter) brings new practical and physical requirements on how to perform dose measurements. By using a silicon detector with a high sensitivity and energy- and angular-independent response, some of the problems were overcome and it was possible the characterize the radiation output from the O-arm system. A holder with a clamp and a flexible ball joint was used. This holder can orientate the radiation detector support and the mover and can be adjusted to hold the detector in a horizontal position. The dose response for three different detectors of different active lengths (0.3, 23.1, and 100 mm) was evaluated for three different beam qualities. Furthermore, the dose profile free in air to control the possible heel effect and width of the X-ray field during rotation was measured, and the dose rate waveform was analyzed. The FWHM of the dose profile was 162 mm. The dose response of the three detectors was reported. The average dose response was lower for the detector with longer active length due to the influence of the dose profile shape. From dynamic measurements, the total exposure time, pulse width, and the number of pulses were verified. In conclusion, an external horizontal hanging holder with a mover option facilitates the dose measurements and enables characterization of the radiation output from the O-arm system.

Figure 17.
A zoom of a part of the radiation waveform output from a O-arm system.

Paper VI: Construction and evaluation of a real-time personal dosemeter based on a Si-sensor invisible to X-rays

The objective was to design a thin, flex card–based personal dosemeter with low angular and energy dependence. It is based on silicon diodes that can measure the personal dose equivalent. Anisotropic conducting adhesive was used to connect the Si sensor to the flex card. Its intended use is for interventional radiology and after nuclear or radiological accidents, as it provides immediate detailed information about the dose rate to the wearer during shorter periods and integrates the dose rate over hours. It can be freely placed anywhere on the body. By placing the dosemeter close to the eyes, it may be possible to estimate the personal dose equivalent as well as the dose at the lens of the eye.

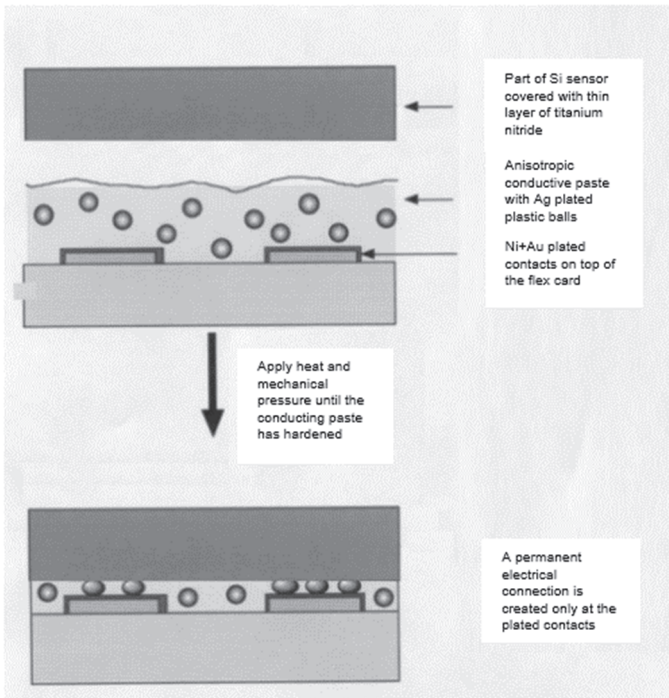

Figure 18.
The principle of how anisotropic conductive paste (ACP) works to connect the sensor to the flex card.

Paper VII: Silicon photomultipliers for medical imaging and dosimetry

Silicon photomultipliers, SiPM (Figure 19), are an enabling solid-state technology for low light sensing, with single photon sensitivity and photon number resolving capability. They feature an extremely high internal gain at the 106 level, comparable to photomultiplier tubes (PMTs), with the advantage of low operating voltage (~50 V compared to ~1000 V for PMT) and low energy consumption. The solid-state technology makes SiPMs compact, insensitive to magnetic fields, and extremely flexible in their design so they can be used in varied applications. The fast development of the multiplication avalanche opens up the possibility of achieving a time resolution at the 30 ps level. Their dynamic range is limited, however, compared to vacuum PMT, and the dark count rate is relatively high, at the current level of 50 kHz/mm^2 at room temperature. Interfaced with scintillation material, SiPMs provide a powerful platform for medical imaging applications (in positron emission tomography/computed tomography and in positron emission tomography/magnetic resonance), for X-ray quality control, and for novel compact radiation protection instruments. This article gives an overview of SiPMs for medical imaging and dosimetry. In addition, a learning and training program targeted to graduate students is described.

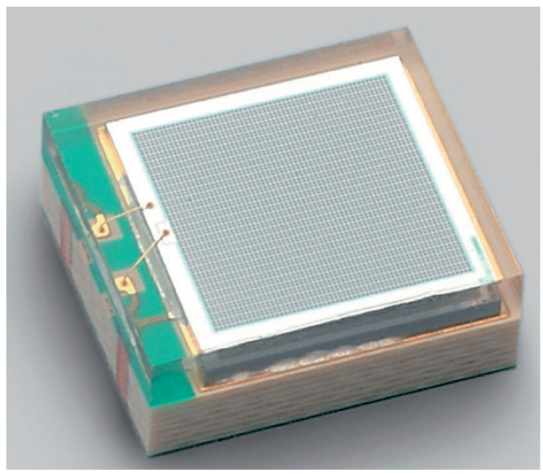

Figure 19.
The S12572-010C boasts a resolution of 90,000 individual avalanche photo diodes (APD) on a 3 mm x 3 mm wafer die, with a pixel pitch of 10 µm. This SIPM is used in **VII** when a high dynamic range is preferred over sensitivity, as is the case with the sensitivity especially needed to measure X-rays.

Discussion and future outlook

There is a great need for new detectors and dosemeters developed for both medical radiology and environmental radiology and for use in the field of radiation protection related to radiological and nuclear accidents and disasters.

This dissertation describes the development of dosimeters by combining and developing two silicon detectors that are already commercially available. 2D R100B (**III**) has a very low energy dependence and 3D CTDP based on the RTI2424 sensor has very low angular dependence (I, IV, V). The choice of silicon as the detector material is also governed by a number of practical considerations.

Therefore, the objectives are to produce an energy-independent, angle-independent 4π detector that inherits the best features of the existing R100B and LH2424 (**I, II, III, IV, V, VI**) and to show advances in new silicon technology (**VII**).

The focus in this thesis is to improve the characteristics of an already existing sensor RTI2424 (**I**) to achieve the energy properties of LH2424 (**IV, VI**).

This was done in the following steps:

- Design a new silicon element and its connector intended for BGA mounting (**IV, VI**)
- Develop an absorption-free contact between the sensor and electrical contact ACA flex card (**IV, VI**)
- Control and test the absorption of contact (**IV**, CTH MC2, LTH 4D Imaging Lab)
- Microfabricate the various parts (**IV**)
- Adapt to thin detectors (**VI**)
- Manufacture a 4π energy filter (**IV**)

Sensors of silicon, sensitive volumes

Silicon is a common element in nature, and silicon technology for the production of semiconductor materials is an industry standard; hence, it is the solid-state material that is the least expensive to produce and is most available for locally developed sensors.

The sensor described in **I** was used in the CTDP detector, where the sensor element is RTI2424, and a wire bonding method was used to contact it to the circuit board. Applications are found in **II**, **III**, and **V**.

A new sensor, LH2424, was designed (**IV**, **VI**) to handle an alternative contact method based on anisotropic conductive adhesive ACA in form of ACP connected to a thin flex card. This makes it possible construct a 4π 3D detector should the wire bonding method not be possible. Ti and TiN was used to provide good contact to ADP on both sides of the sensor, with 300 nm on the contact side and 200 nm on the backside. The TiN protects the surface from oxidation so that a good electrical contact is preserved. This is not the case for the RTI2424, where the surface instead is covered by a thin layer of aluminum that oxidizes over time.

A sketch of the present LH2424 sensor based on a 350 high-purity silicon waver is presented (Figure 20).

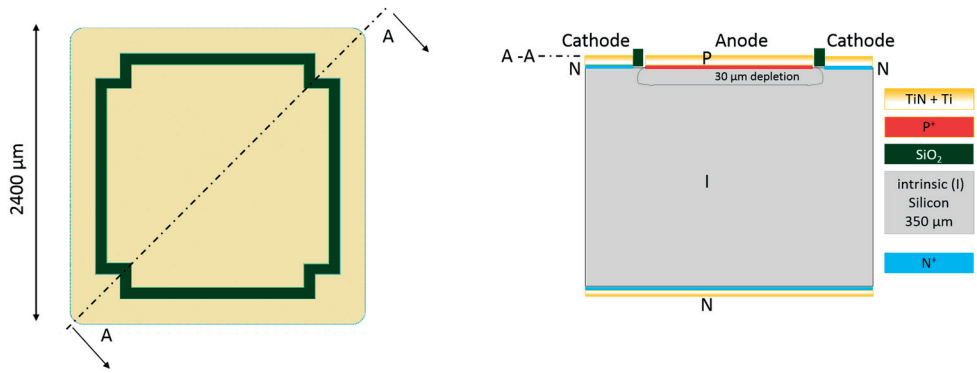

Figure 20.
LH2424 PIN sensor. (Left) 2.40 mm x 2.40 mm from contact side. (Right) Sketch describing the structure and the layers needed to make an electrical contact via the use of ACP and the thin flex card.

The absence of encapsulation of the RTI2424 sensor and the position of the contact on only one side is an important prerequisite for constructing a “spectrometric” detector with minimal self-filtration. This property is demonstrated in **II**. In the

future, one can anticipate a need for radiation detectors to detect individual photons and their energy (Figure 7).

This will be significantly more common in all evolving developments (Åslund *et al.* 2007, Ballabriga Suné 2010). Spectrometric imaging can be designed to achieve low-noise images and multidimensional "energy images" instead of an energy-integrated intensity picture.

One disadvantage of using silicon is its atomic number. Primarily, it is higher than the atomic number of human tissues, which complicates its use for dosimetry. On the other hand, with a higher atomic number, the detector signal would be higher. This can partly be compensated for by placing the silicon sensors on the high edge to obtain a thicker detector.

An advantage of silicon is that the mobility of the charge carriers is high compared with other solid-state materials, e.g., CdTe (Bornefalk *et al.* 2010). This is a way to avoid pileup effects for high-dose rate beams such as those from CT.

Article **I** shows a unique way to measure the sensitivity volume of the detector. This is basic information to correctly simulate the performance of the sensor using Monte Carlo simulations. The same sensitivity volume was found for three different X-ray beam qualities: 28, 70, and 120 kV (**I**).

As stated in the introduction, the objective was also to develop better dosemeters for radiation protection and emergency preparedness (Herrnsdorf 2012, Ören *et al.* 2016, **VI**). Thus, there is the need to combine small, angle-independent thin sensors, for example, for eye dosimetry (**VI**), with sensors that have a significantly higher sensitivity and additionally spectral properties. (Herrnsdorf 2012, **VI, VII**).

To increase the sensitivity range, semiconductor photomultiplication detectors (SiPM) can be used (**VII**). Because this detector has a "built-in gain" of up to a million compared with a conventional PIN sensor and also shows the ability to measure the energy of individual photons, this technology is clearly future oriented and useful when high sensitivity and low dose levels occur. SiPM has a very short pulse response and has already been used in applications in PET, PET/MR, and radiation protection instruments (**VII**). Applications for this technique are large and extend outside health care. They include measurements around installations such as MAX-IV and ESS, including neutron measurement (**VII**).

Wire bonding vs. ACA and flex card

It is important to keep the sensor clean enough of interfering materials so that the detector can be used for spectrometry without elements with absorption peaks other

than those from silicon (**I, II, IV, VII**). Since this is a competing requirement for achieving a good contact—usually done by soldering, surface mounting, or wire bonding—this was a major challenge. The existing RTI2424 sensor (**I**) already has aluminum layers on both sides protect the silicon and to enable wire bonding. Over time, a nonconductive oxide is formed and constitutes an isolation layer. The Al_2O_3 layer can be penetrated using wire bonding, which "ultrasonically wipes" the surface and creates contact through the Al_2O_3. To avoid bonding techniques that use high-Z materials, contact surfaces that do not oxidize and additionally have low photon attenuation were used in the new sensor, LH2424. This sensor has one side adapted for oxide-free contacts at five points based on ACP as contact material (Bazilchuk *et al.* 2016) and is as lightweight as possible since it uses titanium (Ti-TiN) instead of Au (Figure 10).

The reasons for abandoning wire bonding are that it has high absorption, cannot be uniquely placed, is expensive to assemble, and is mechanically sensitive as the wires are on the order of 50 µm and their length is limited. If the LH2424 is to be enclosed in a 3D metal filter, it is practically impossible to use wire bonding since the wires cannot be isolated against the leading 3D metal surface.

The solution for contacting the sensor to the flex card has a very little impact of X ray attenuation (Figure 21).

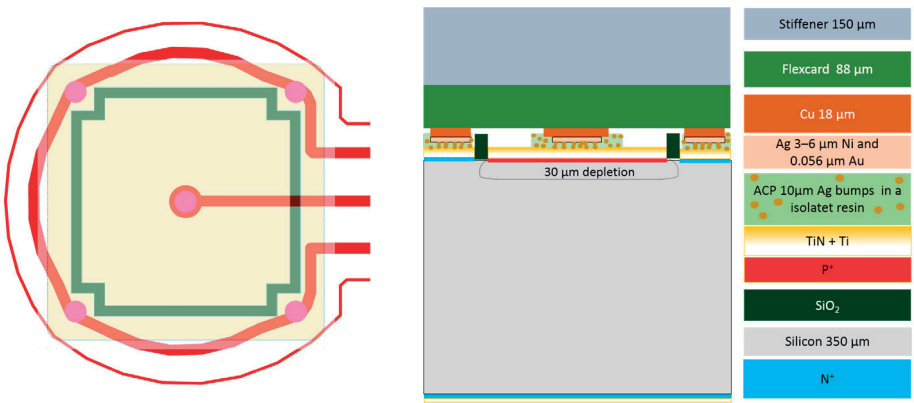

Figure 21.
(Left) Flex card at the sensor side with the 5 contact points. (Right) Microscope image of a LH2424 sensor where the ACP small Ag bumps can be seen (8–20 µm size).

Articles **IV** and **VI** show the use of ACA in the form of a paste. This method is widely used in smartphone manufacturing and in the production of thin credit cards (Nguyen 2016). It allows for a lower temperature and higher 3D packing density as well as a mechanical fixation at a single point between the connectors; however, for

radiation detection, it has another very important function as it significantly reduces the density of high-Z material in the contact surfaces compared to conventional connecting technology (**IV**) (Figure 21). In addition, modern microfabrication enables the use of assembly robots that can dispense the paste automatically in combination with “pick and place” equipment for rational manufacturing.

Energy filter design

The design of the energy filter is of outmost importance for the energy response of the dosemeter. One must always consider whether it is possible to manufacture a 4π dosemeter that is small enough to be used in existing QC phantoms. For CT, the maximum diameter is 12.5 mm. The initial evaluation and contacts in the early work indicated that it may be possible to fabricate micro metal filters with a resolution down to 35 µm or less. This high resolution is a prerequisite for a sufficiently detailed 3D filter and the use of the detailed Monte Carlo simulation of the hole structure for energy and directional independence (**IV, VI**); see Figure 22.

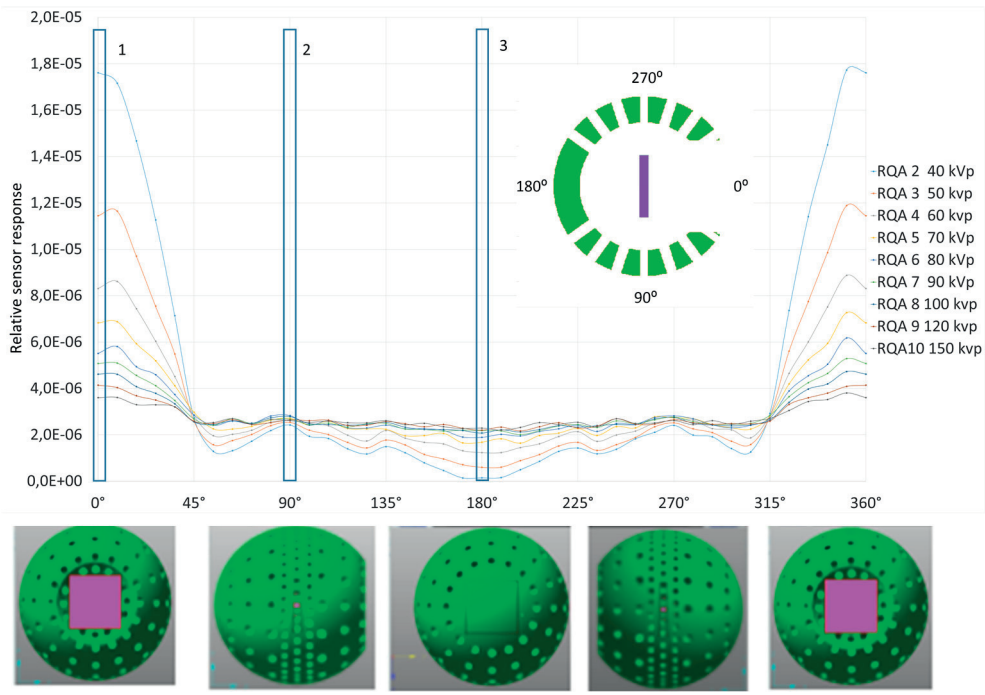

Figure 22.
Demonstration example to show the importance of selecting the right hole pattern to reduce energy dependence.

Figure 22 shows that, in the same simulation, three measured ROIs of the energy filters 1, 2, and 3 result depending on the angle of the incoming X-ray beam. This illustrates the energy dependence due to hole pattern. The same filters were simulated at 0° and no filter (1), 90° (2) (hole), and 180° (3) with only metal.

From the graph data, the lowest energy dependence can only be achieved with a combination of partly radiated detector (90° and 270°). This is shown as the different energy distributions coincide on the vertical axes. Furthermore, as a result, the ratio between ROI 1 and 2 shows that a much lower signal can be expected when an energy filter is used.

The hole pattern of the energy filter was designed so that the correction of the energy dependence should be balanced over the surface and the corresponding "active" sensor area independent of the X-ray source position (in 4π). This design was based on an earlier initial selection of hole size, thickness, and distribution around the sphere (Figure 23).

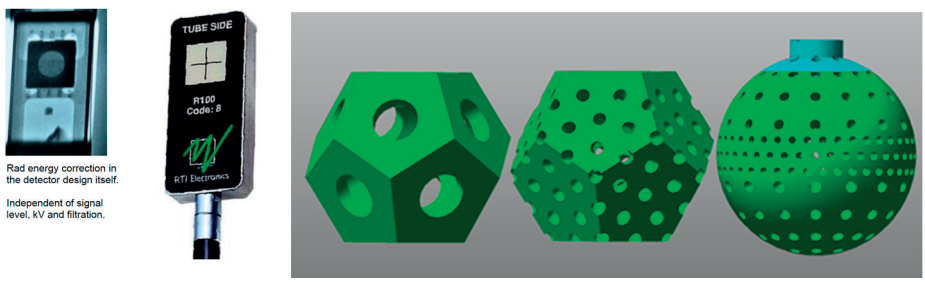

Figure 23.
The evolution from the basic two-dimensional energy filter to an increasingly sophisticated version of the 3D 4π energy filter in **IV**.

Iterative MC simulations provided feedback for modifying the 3D CAD model until the results achieved energy dependence, less than 5% for the IEC beam qualities RQR and RQT in the range of 65–145 kV. Furthermore, due to the rotational symmetry of the sensor in the x- and y-directions, the hole pattern was repeated around the z-axis. Therefore, it was not necessary to verify all possible combinations of the response of the hole pattern as a function of the beam qualities RQX and the rotation angles α and ß (f(RQX,α,ß)) (**IV**).

From earlier simulation results with only the sensor present (**IV**), the most significant changes in the sensor response were for ß = 90° and 270° for a 360° rotation in α. For these angles, the sensor area has a minimum as it varied from 2.4 × 2.4 mm^2 to 2.4 × 0.35 mm^2 when α is rotated one complete turn in the direction from the source. This indicates that it is sufficient to simulate a limited number of combinations of (f(RQX,α,ß)).

Currently, the best and most practical manageable design of the spherical energy filter (EFR) has an outer diameter of 7.0 mm and 285 holes in total. One hundred and twenty holes (around ß=0) have a diameter of 0.28 mm, and the remaining 138 holes, evenly distributed over the rest of the sphere, have a diameter of 0.40 mm (Figure 10, Figure 24).

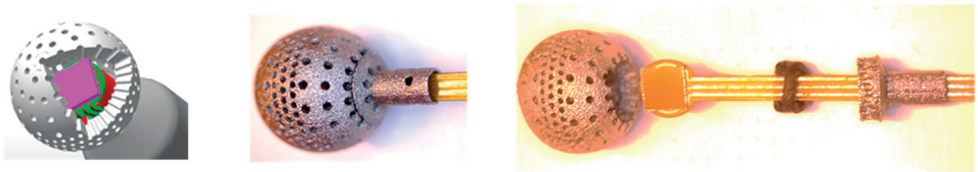

Figure 24. Optimized energy and angular filter.
(Left) CAD model. (Middle) 3D printed version of the 4π dosemeter. (Right) Dosemeter assembly parts: “Head” part of the filter, sensor mounted on the flex card, detector holder, and “neck” part of the energy filter **IV**.

Final approach of dosemeters

Depending on the application, the dosemeter can be mounted without a 4π energy filter in order to measure freely in air as a radiation protection dosemeter or for spectrometry (Figure 25(1)) when the bare sensor is the preferred choice. Otherwise, it can be part of a CT/CBCT application (**V**) (Figure 25(2)) or "open" for 4π radiation (**IV**) at the end of the assembly (Figure 25(3)).

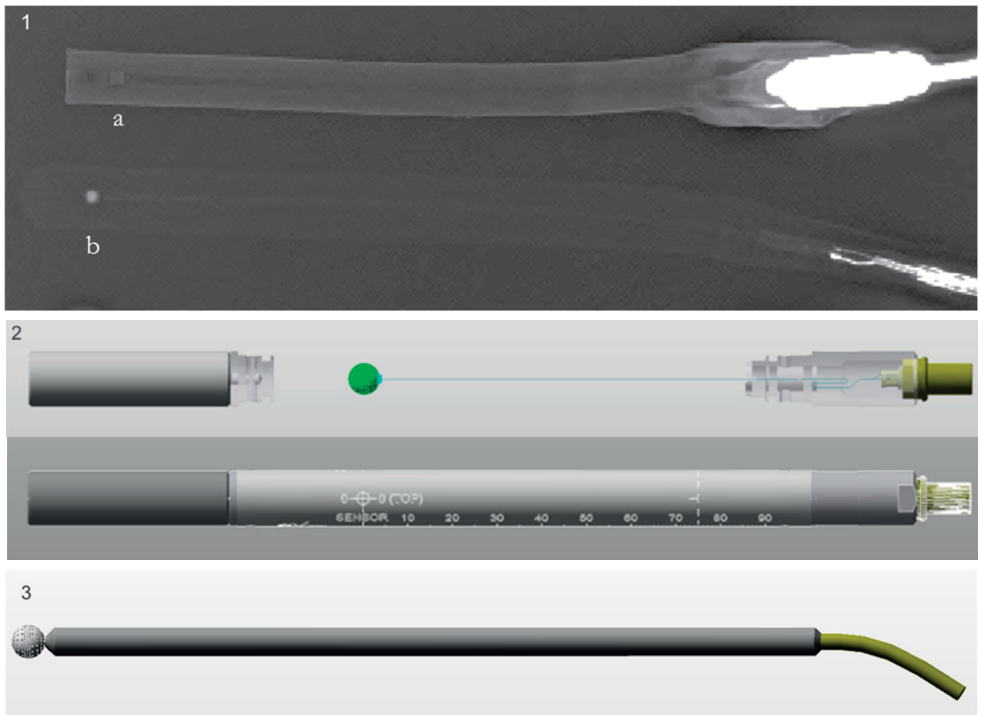

Figure 25.
(1)The dosemeter without 4π energy filter: (a) bare sensor, (b) with a thin filter mounted on both sides (**VI**).
(2) 4π dosemeter within a CT/CBCT assembly. (3) 4π Dosemeter as a reference detector.

Micro assembly of the sensor and the energy filter

Since the parts involved are of sub-mm size, their manufacturing and assembly are challenging. This is especially valid for the mounting of the 4π dosemeter (**IV).**

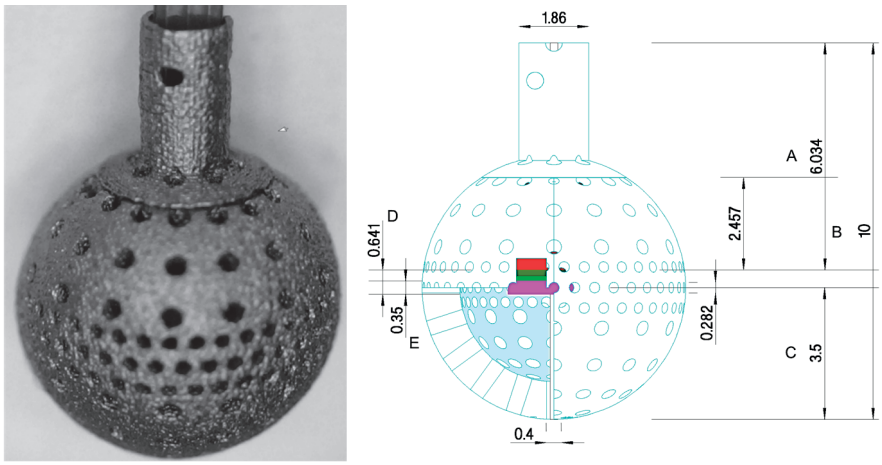

Figure 26. Assembly of the sensor with flex card detector holder and energy filter.
Assembly of the sensor with flex card detector holder and energy filter. A, B, C, D, and E refer to Table 3. (Left) The energy filters with two parts put together. (Right) The nominal dimensions indicated in mm. The pink rectangle is the sensor that can partly be seen in the opened segment of the sphere's mantle surface. See also Figure 24 for an additional image of the parts inside the 4π energy filter.

Importance questions are raised and are answered in the following text:

- Can the small part be produced with enough accuracy to guarantee the calculated energy and angular independence?
- How can it be guaranteed that the sensor is located in the center of the 4π filter?
- How can the relative position and angle of the assembly of the parts be checked?

The mounting method that is suggested is to put the four parts (sensor, flex card, plastic holder, neck, and head part of the filter) together (Figure 26). Since the three first parts are placed inside the head part of the filter, the actual position of the sensor relative the center of the filter cannot be measured directly. Instead, an approach based on an indirect measurement of well-defined surfaces is made. Then, the position of the sensor is calculated. The detector holder is then milled to correct its dimension so that the sensor is positioned in the center of the energy filter.

Table 3. List of parts that are involved in the assembly of the silicon detector and 4π filter:

Item	Parts and nominal and measured values (mm)	Nominal	Measured	Note
B	Total height, stainless steel neck + head (when brought together)	10.000	10.000	Figure 26 right
Ainit	Initially total height neck+detector holder	6.034	6.100	Figure 26 right
C	Ø/2 stainless steel head EF07 (measured across the head diameter/2)	3.500	3.515	Figure 26 right
E	LH2424 2.45x2.45 sensor thickness	0.350	0.350	Figure 26right
D	Thickness sensor+flex card with stiffener sensor side	0.641	0.620	Figure26 right
Corr A	Ainit-(B-(C-E/2)-D)	0.000	0.060	60 µm must be milled away
3	Example of the resolution obtained for measurement Ø inner dimensions stainless steel neck EF07	1.570	1.5752	Figure 27 and Figure 28 (left top)
	Hole energy filter EFR	0.40	0.30	Earlier design
	Hole energy filter EF07	0.40	0.37	Present design

As can be seen from Table 3, the measured values were near the nominal values from the 3D CAD. As an example, the original version EFR had 0.30 holes when it should be 0.40.

Figure 27 displays the wall of the neck part of the energy filter (as can be seen in Figure 28(left top)). The surface is rough in this scale. Actually, 0.37 mm measured with a calibrated steel needle is misleading and the diameter is practically 0.40 mm.

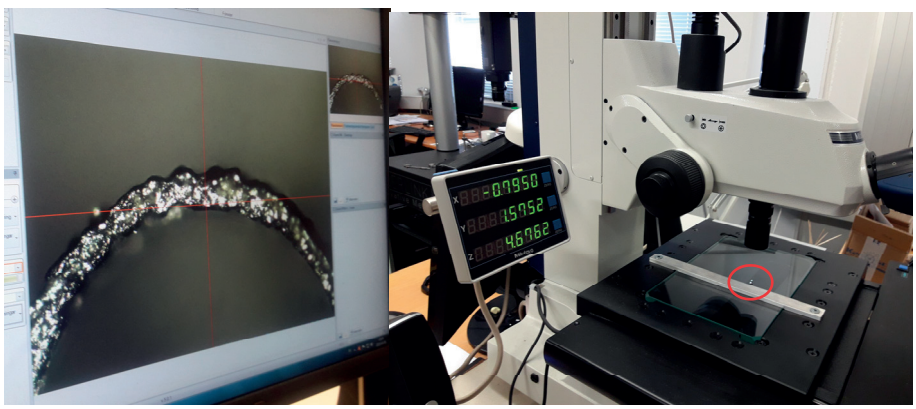

Figure 27. 0.5 µm resolution contactless microscope.
(Left) The structure of the neck energy wall. (Right) The measurement resolution is 1.5752 mm for the sample 3 of the neck energy inner dimension (marked with a red circle in the figure), (see Table 3, row 7).

Now, all dimensions are known and the correction of the height of the detector holder can be calculated: CorrA=A_{init}-(B-(C-E/2)-D) mm. The corrections in mm must be milled away from the plastic holder by setting up the detector holder + energy filter neck part in the same equipment that was originally used to make the detector holder. The equipment used is shown in Figures 27 and 28.

The final assembly of the sensor to the flex card is made with a round teflon rod (Figure 28) with a milled hole 0.175 mm in depth. This hole aligns the sensor's four corners to the detector holder using the same watchmaker lathe as in Figure 28 (down right), with glue between the flex card side and the top of the detector holder. The flex card is then threaded through the detector holder support and within the neck part (Figure 29).

Now, the sensor's midpoint should be in correct position within the 4π energy filter based on the earlier indirect measurement.

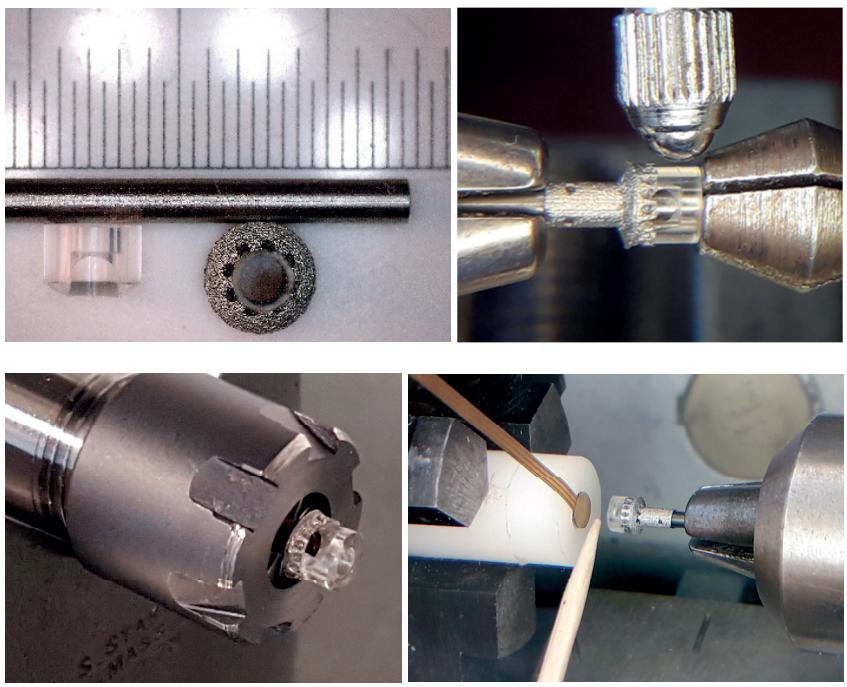

Figure 28.
(Left top) PMMA detector holder, neck part of energy filter. A guide pin is shown to align (right) the detector holder and the neck part using a watchmaker lathe and a dial indicator to glue the parts together. (Left down) The setup to mill the detector holder to its final height and flatness on the neck part of the energy filter. The precision of this micro milling equipment is within 0.5 µm. (Right down) An image of the cylindrical guide rod that fits the square sensor precisely and guides the sensor with its flex card in the center of the detector holder.

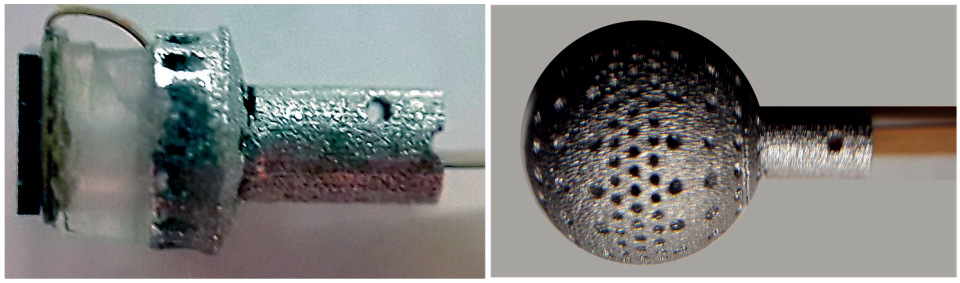

Figure 29.
Left:Sensor and flex card after glued to the detector holder and the flex card mounted inside the neck part. Right: The head and neck part joined together. The diameter of the head part is nominally 7.00 mm.

In the future, the detector holder and the neck part of the filter should have the same dimensions so that the alignment pin can align both parts with higher precision when glued together. Furthermore, this will make it easier for the flex card to pass through the hole in the neck part of the energy filter. It is also important to use an assembly robot to dispense the glue and to do the “pick and place” work to align and fixate the parts as well as to steer the precision mill, watchmaker lathe, and precision measuring board.

Future applications and developments

The SiPM technology appeared about 15 years ago and are still rapidly evolving. The interest in this class of detectors and the number of applications based on SiPM are confirming that we are at the edge of a revolution. The SiPM technology can be anticipated to have a major impact in the fields of medical imaging, quality control, dosimetry, radiological and nuclear emergency preparedness, as well as automotive and analytical techniques for biology and biotechnology. New SiPM based dosemeters have already found their way out on the market (**VII**).

It is essential to train and educate graduate students about SiPM technology in a cross-disciplinary environment to promote their knowledge-based imagination and creativity. Various examples of applications are illustrated during a course held annually at the Medical radiation physics in Malmö (Figure 30).

The costs for SiPM is decreasing and is now comparable to vacuum tube PM based systems. The small measuring area and higher background count rate are however still not in parity to those of traditional PM tubes. Scintillators optically coupled, directly or via light guides, to SiPMs are used to construct large detectors. Coincidence registration can be used to minimize the background count rate. Two examples of its use can be found (Hudin *et al.* 2012, Krona 2015).

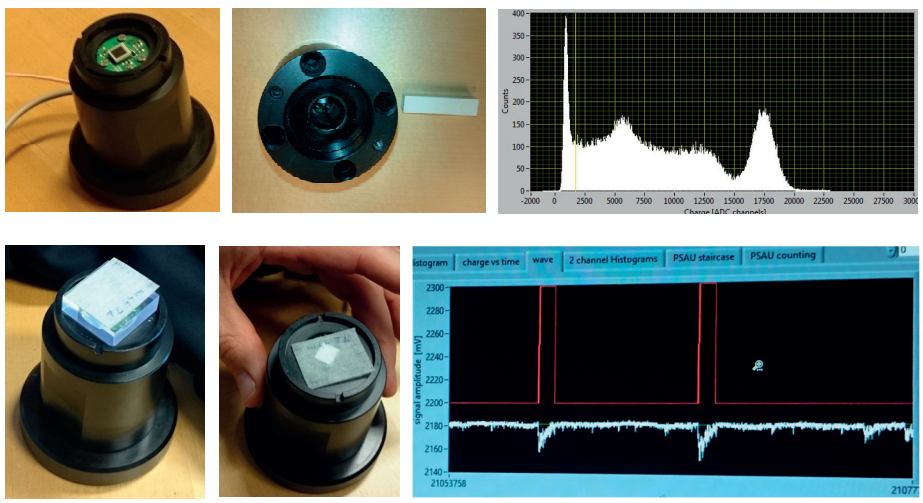

Figure 30
Application with SIPM for measurements of pulse height distributions from scintillators, intensifying screens and for luminince dosemeters as OSL.

While traditional PM tubes technology is mature, SiPM has a high potential for development. Figure 31 illustrates the rapid evolution between 2014 and 2016.

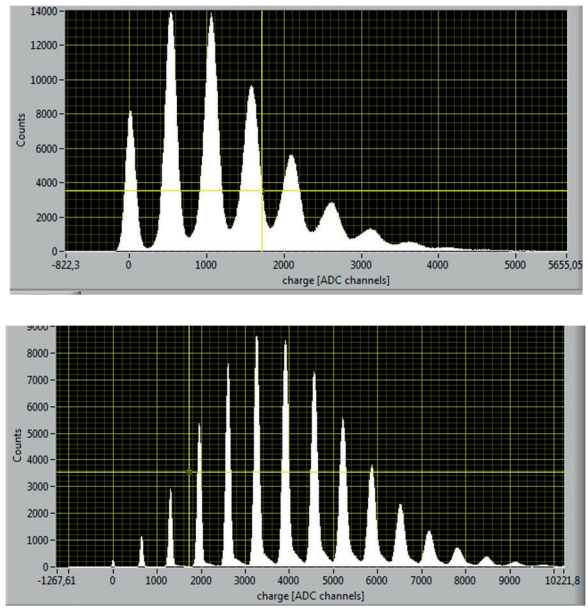

Figure 31.
Comparison between an old 1 x 1 mm2 Hamamatsu SiPM (model S10362-11-025C) (top) and a new 1.3 × 1.3 mm2 Hamamatsu SiPM (model S13360 -1350CS) (bottom).

Systems based on SiPM and Si sensors are more lightweight, less power consuming and rugged than Ge spectrometers and system based on PM tubes. This makes them more mobile and thus of high interest for *in situ* measurements (Figure 32).

Figure 32.
Drone inspection with mobile battery operated 4π dosemeter or/and SiPM alpha/beta/gamma/neutron spectrometer/dosemeter

There are also a number of other applications for the dosemeter described in **VI.** As it is thin, it can be used as an active alternative to passive TL- and OSL-dosemeters (Figure 33).

Figure 33.
The real time personal dosemeter based on a Si-sensor described in **VI** In this application the thin sensor and flexcard is placed inside the phantom where normally only TLD and OSL could be placed.

Concerning the status of the 4π dosemeter, described in **IV**, the first prototypes have been fabricated and the performance will be verified against the result of the Monte Carlo calculations. Minor adjustments of the hole pattern and fine tuning of the micro assembly might be needed.

There are also a number of applications for the dosemeter described in **IV**.

Together with its already described use as a QC dosemeter for CT/CBCT and tomosynthesis systems, an important future application for this dosemeter is for validation of software driven dosemeter systems (Figure 34).

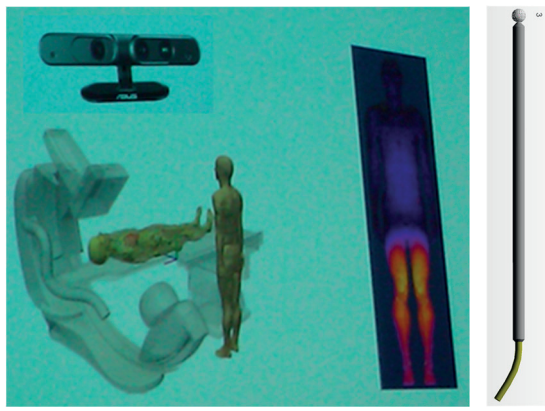

Figure 34.
4π dosemeter for QC of CT- and CBCT-units. Monte Carlo driven control of the dose to patient and personnel in an X-ray room.

One example of an application that meets the aim set for the 4π dosemeter in the introduction is shown in Figure 35.

The setup illustrates the measurements of the exit and entrance dose value using the same single dosemeter dynamically when the CT is rotating. The first high pulse is the entrance dose pulse measured when the X-ray tube is just below the dosemeter and 500 ms later, the exit dose pulse is measured with the same dosemeter.

The energy absorbed in the phantom can be calculated from the difference between the two dose values. To be able to measure the dose correctly a combination is needed of high spatial, temporal resolution, and low energy and angular dependence. That is the aim for the 4π dosemeter.

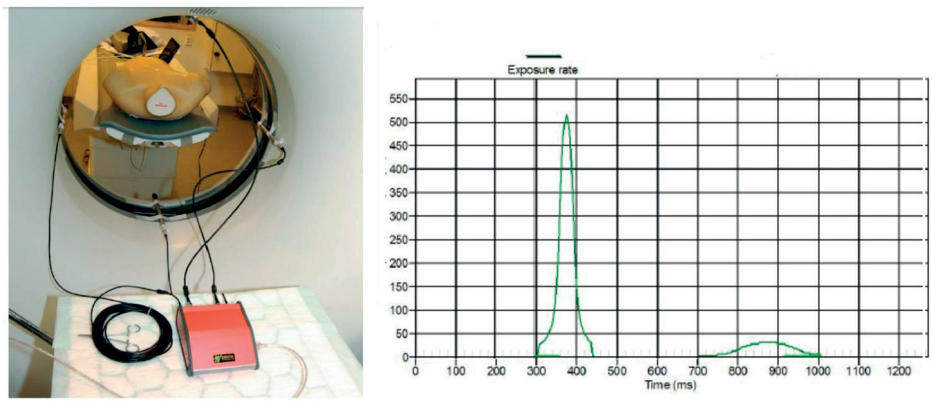

Figure 35. Virtual KAP meter.
The left figure displays a set up in a CT were the dose is measured in, 0˚,90˚,180˚ and 270˚ position simultenously around a body anthropomorphic phantom using a Barracuda multi channel electrometer (RTI Group). For the lowest dosemeter (0˚), that is the only one needed, the doserate vaweform is displayed on the right picture. The CT is rotating one turn per second so the the time between the dosemeter doserate pulses is 500 ms.

Summary and conclusions

In this thesis, a silicon sensor was adapted for absorbed dose measurements by optimizing the electrical contacts with the sensor and its flex card. This avoids interfering high-Z materials and uses anisotropic conductive adhesive (ACA) contacts. To get a signal that is independent of the energy and direction of the photons reaching the detector (sensor, ACA, and flex card), a stainless steel filter was designed and manufactured to encapsulate the silicon detector. To achieve an energy and directional response which is as uniform as possible for various radiation qualities and beam directions, the filter was designed using a series of Monte Carlo calculations. The hole pattern is designed so that the energy dependence correction should be balanced over the surface; then, the corresponding "active" sensor area is similarly independent of the X-ray source position (in 4π). The energy filter and its hole pattern were created using additive manufacturing (AM) in the form of metal 3D printing. The functionality of the dosemeter was verified by simulation to fulfill the quality criterion of energy dependence being less than 5% for the IEC beam qualities RQR and RQT in the range of 65–145 kV.

The avoidance of disturbing materials around the sensor also opens the possibility for energy dispersive measurements. It was even shown to work as an α-spectrometer.

In the future, there will likely be a need for radiation detectors for individual photons and for diagnostic X-rays. If sophisticated ASICS with both preamplifiers and high-speed ADC/MCA are used to directly measure the sensor charge pulse, even a high dynamic dose rate from, e.g., CT can be collected with controllable pileup.

A combination of high spatial and temporal resolution, combined with high sensitivity, low energy, and angular dependence, has been shown to be valuable for correct monitoring of the dose rate, for the dosimetry of small organs such as the eye lens, and for mapping dose gradients in diagnostics as well as in radiation therapy.

A real-time personal dosemeter was constructed. In radiation protection, active dosemeters that continuously show the dose rate for the wearer allow users to

change procedures and positions and thus reduce their absorbed dose. Such dosemeters can also be used to test radiation protection arrangements such as protection glasses and screens and to find radiation “hot spots.” Similar needs exist in radiation emergency situations. The involved personnel have the need for immediate information about their absorbed dose rate so they can plan the next step in their work.

Other examples of the potential of dosemeters with a combination of high spatial and temporal resolution is illustrated by the possibility of determining dose profiles, the dose per pulse, and the beam current variations.

The thesis also identifies the need to use the potential of SiPM detectors as an alternative to vacuum PM tubes for improved sensitivity and spectroscopic possibilities.

Acknowledgements

I want to express my sincere gratitude and appreciation to all people who have helped and supported accomplish this thesis.

I would especially like to thank:

- My mother Ann, who raised my interest to try to improve healthcare.
- Sten Carlsson, who in 1979 presented for me what turned out to be my destiny, the rest of my life, and teached me the great joy and strength of combining education and work.
- Hans Forsberg, my great mentor and friend who 1987 wrote the Swedish QA standard for X-ray equipment maintenance: organization, content and implementation.
- Cynthia H. McCollough, Ph.D., Radiological Department, Mayo Clinic, USA who explained the need for better dose detectors and especially for an energy-independent 4π detector and for dose profile measurements for QA on CT / CBCT systems.
- Pei-Jan Paul Lin, Ph.D. Professor and Chair - Radiation Physics and Biology, Virginia Commonwealth University Medical Center, USA who gave me the possibility to work with modern wide beam CT systems.
- Andreu Badal and my other friends at FDA, USA and IEC CT Working Group who convinced me at an early stage, that it would be possible to perform realistic MC calculations on the small detectors that I wanted to create.

My sincere appreciation and gratitude goes to my supervisors for the scientific advice and discussions where we had so much fun:

- Mikael Gunnarsson, who always stood up for me and with a careful hand, made me more efficient (especially when Sören was not there.)
- Sören Mattsson, who did not give up on me even before I started studying to this Ph.D. His talent to inspire is an important reason to have managed six years of part time study. Thanks for a nice research environment. Sören also introduced me to the radiation protection field and other dosimetry directions with his cutting-edge skills.
- Göran Thungström, with knowledge and wisdom, taught me what is worth knowing about silicon sensors.
- Martin Andersson has always been there, been a great friend and helped me keep up to date.

My co-authors:

- Göran, Marcus, Ünal, Hannie, Massimo, Martin, Mikael and Sören.

Other important people who make my job possible:

- Professor Christer Fröjdh, Department of Electronics Design, Mid University, Sundsvall, Sweden. Thank you Christer and your team in northern Sweden who have been so kind to open your knowledge and introduce me to your excellent micro focus x-ray lab, cleanroom facility and the knowledge of Medipix technology.
- Professor Massimo Caccia, Dipartimento di Scienza e Alta Tecnologia, Universidad degli Studi dell'Insubria, Como, Italy. Massimo, with great enthusiasm and wisdom and practicality, introduced me to next generation SiPM radiation protection sensors and luminance dosemeters.
- Professor Johan Liu, Micro Technology and Nanoscience (MC2), CTH, Gothenburg, Sweden. Thanks Johan, that you allowed me to stay 8 months of research time and introduced me to ACA and Microelectronics.
- Professors Martin Bech and Stephen Hall who let me participate in the imaging research school to learn how to find applications for the use of MAX IV and other image management facilities. And especially Stephen, who gave me the opportunity to test different versions of the sensor in the 4d image lab in Lund.
- Medical Physicist Jan Lindström for his good friendship and thinking outside the box

- All my colleagues, especially Martin, Marcus and Hannie, who I worked closest to during my six years in Malmö and Skåne University Hospital, my professor Lars E Olsson, Vivéca, Daniel, Magnus, Maria, Lena, Lovisa, Emilie, Simon, Sara B, Kai, Karl, Cecilia, Hanna, Anja, Anders T and really all. No one should feel omitted.
- Friends at Hamamatsu, Digital Metal, MidDec, Note and Hagema who gave me good advice.
- My friends at RTI Group who let me do this project, and especially Ulf Toll, and Rob Morrison with whom I share many good memories at the beginning of my career.

This survey was supported financially by the Radiation Safety Authority (SSM) (SSM 2012-2131, SSM 2013-1436 and 2013-1437) and helped to launch this project.

I would also like to thank the RTI group that financed the insurance required at MC2, CTH during the 8 month stay in 2013.

And after this long list, I would like to mention my sister Magdalena, her daughter Nora and my father Klaus, who has always been there for me. I hope now that I can do other things, including having more time with my first grandchild.

Bibliography

Andersson M., Herrnsdorf L., Mattsson S. 2017. IDAC-CAD2VOX - A software for radiation protection calculations for the ICRP reference phantoms which are in an environment described by detailed cad drawings. *In: Medical Physics in the Baltic States 13 (edited by Adlienė D) Kaunas University of Technology*, pp 10-13.

Ballabriga Suñé R. 2010. The design and implementation in 0.13 µm CMOS implementation algorithm permitting spectroscopic imaging with high spatial resolution for hybrid pixel detectors. *CERN-THESIS-2010-055*

Bazilchuk M, Pettersen S, Kristiansen H, Zhang Z, and He J. 2016 Electromechanical characterization of individual micron-sized metal coated polymer. *Journal of Applied Physics 119, 245102*

Bengtsson T, Herrnsdorf L 2013. High resolution pulse measurements. Practical examples. *In: PTB Seminar Strahlenschutzdosimetrie in gepulsten Photonen-Strahlungsfeldern – Teil 2*, *18-19* November 2013

Boone J M. 2011. New advances in CT dosimetry. *https://www.aapm.org/meetings/amos2/pdf/60-14863-35661-83.pdf.*

Bornefalk H, Danielsson M 2010. Photon-counting spectral computed tomography using silicon strip detectors: a feasibility study. *Phys. Med. Biol 55, 1999-2028.*

Cao L, Li S, Lai Z, Liu J. 2005. Formulation and characterization of anisotropic conductive adhesive paste for microelectronics packaging applications. *J Electr Materials 34(11), 1420-1427.*

Castoldi A. 2011. Signal formation in radiation detectors: Ramo's theorem and its application to practical cases, Politecnico di Milano & INFN, Sez. Milano, *Advanced School and Workshop on Nuclear Physics Signal Processing, November 21-24, 2011, Acireale (CT), Italy.*

Digital Metal. 2018. High-precision Additive Manufacturing technology from a metal powder giant Vol. 4 No. 1 © Inovar Communications Ltd *Metal Additive Manufacturing, 103-111.*

EU. 2014. Medical radiation exposure of the European population, Part 1/2. Radiation Protection No180, *Publication Office of the European Union*.

Herrnsdorf L**,** Månsson L G, Strid K-G. 1984. Design and performance evaluation of a new instrument for in-beam quality control of X-ray equipment. *Report GU-RADFYS 84:09 (1984) Department of Radiation Physics, University of Göteborg, Sahlgenska Hospital, Göteborg, Sweden.*

Herrnsdorf, L. 2012. A directly readable personal dosemeter for radiation emergemcy situations – A design approach*. In: Medical Physics in the Baltic States 10 (Ed. By Adliene D), Kaunas University of Technology*, *pp 23-28.*

Hudin N, Pinot L., Charon Y, Dinu N, Ait T, Imando, *et al.* 2012. Development of intra-operative beta probes based on silicon photomultipliers. *International workshop on New Photon-Detectors, LAL Orsay, France.*

ICRP. 2015. Radiological protection in cone beam computed tomography (CBCT). ICRP Publication 129. *Ann ICRP 44(1)*

IEC. 2005. Medical diagnostic X-ray equipment – Radiation conditions for use in the determination of characteristics. *IEC 61267, 2005*

IEC. 2012. Particular requirements for a basic safety and essential performance of X-ray equipment for computed tomography. *IEC 6060601-2-44:Edition 3.0 Amendment 1, 2012-08.*

IEC. 2012. Medical Electrical Equipment – Dosimeters with Ionization Chambers and/or Semi-conductor Detectors as used in X-Ray Diagnostic Imaging, *IEC-61674:2012, IEC, Geneva (2012).*

Krona D. 2015. Development of a portable beta-spectrometer for in situ measurements of Sr-90 and Y-90, *Master of Science Thesis, Medical Radiation Physics Malmö, Department of Translational Medicine, Lund University*, (37p)

Lin P, Herrnsdorf L. 2010. Pseudohelical scan for the dose profile measurements of 160-mm-wide cone-beam MDCT. *Am. J. Radiol. 194, 897-902*

Lindström J. 2016. The non-invasive X-ray multimeter principles, advantages, drawbacks and uncertainties. *Booklet for the Course "Physics of Diagnostic Radiology" Karolinska universitetssjukhuset, Solna, Sweden*.

Mattsson S. 2016. Need for individual cancer risk estimates in X-ray and nuclear medicine imaging. *Radiat Prot Dosim 169(1-4),11-16.*

Nguyen, H. 2016. A study of Anisotropic Conductive Adhesives with Novel Spacer Particles , *Ph.D thesis, Faculty of Technology and Maritime Science University College of Southeast Norway*.

Persson M, Huber B, Karlsson S, Liu X, Chen H, Xu C, Yveborg M, Bornefalk H, Danielsson M. 2014. Energy-resolved CT imaging with a photon-counting silicon-strip detector. *Phys. Med. Biol.* 59, 6709-6727.

Rauch, P, Lin, P. -J. P., Balter, S., Fukuda, A., Goode, A., Hartwell, G., LaFrance, T., Nickoloff, E., Shepard, J. and Strauss, K. 2012. Functionality and operation of fluoroscopic automatic brightness control/automatic dose rate control logic in modern cardiovascular and interventional angiography systems: a AAPM report of Task Group 125 Radiography/Fluoroscopy Subcommittee, Imaging Physics Committee, Science Council. *Med. Phys. 39, 2826–2828.*

Rehani M, Holmberg O, Ortiz Lopez P, Mettler F. 2011. International action plan on the radiation protection of patients. *Rad Prot Dosim 147(1-2) pp 38-42*

RTI. 2010. http://rtigroup.com/content/downloads/application-notes/Dose%20Probe%20-%20Energy%20Correction%20Factors%20for%20R100B-PDP%20-%20AN010.pdf, http://rtigroup.com/content/downloads/application-notes/Dose%20Probe%20-%20Energy%20Correction%20for%20R100B-PDP%20for%20Cu%20filtration%20-%20AN017.pdf (last accessed 28 April 2018).

Thungström G, Herrnsdorf L, Norlin B, Reza S, Krapohl D, Mattsson S, Gunnarsson. 2012. Measurement of the sensitive profile in a solid state silicon detector, irradiated by X-rays. *14th International Workshop on Radiation Imaging Detectors, 1–5 July, Figueira da Foz, Portugal*

X-5 Monte Carlo Team. 2003. MCNP-A General Monte Carlo N-Particle Transport Code, Version 5. *LA-UR-03-1987*.

Åslund M, Cederström B, Lundqvist M, Danielsson M. 2007. Physical characterization of scanning photon counting digital mammography system based on Si-strip detectors. *Med. Phys. 34(6), 1918-1925*.

Ören Ü, Nilsson J, Herrnsdorf L, Rääf C.L, Mattsson S. 2016a. Silicon diode as an alpha particle detector and spectrometer for direct field measurements. *Radiat. Prot. Dosim. 170(1-4), 247-251.*

Ören, Ü, Herrnsdorf L, Gunnarsson M, Mattsson S,Rääf C.L. 2016b. Can an energy-compensated solid-state X-ray detector be used for radiation protection applications at higher photon energies? *Radiat. Prot. Dosim. 169(1-4), 192-196.*